DETERMINING EVAPOTRANSPIRATION AND CROP COEFFICIENT VALUES USING AN ADJUSTED PENMAN-MONTEITH EQUATION OVER CANOLA (*Brassica napus*) IN SOUTHERN MANITOBA

By

TONY A. BRITTON

A Thesis submitted to the Faculty of Graduate Studies of the University of Manitoba in partial fulfillment of the requirements of the degree of

MASTER OF SCIENCE

Department of Soil Science

University of Manitoba

Winnipeg, Manitoba, Canada

ABSTRACT

Britton, Tony Aaron. M.Sc., The University of Manitoba, October, 2019. Determining Evapotranspiration and Crop Coefficient values using an adjusted Penman-Monteith Equation over Canola (*Brassica napus*) in Southern Manitoba. Major Professors; Aaron J. Glenn, Brian D. Amiro.

The FAO-56 Penman-Monteith equation and crop coefficients were adjusted to better represent modern canola (*Brassica napus*) grown in Manitoba at three locations. It was hypothesized that incorporating direct measurements of available energy, developing crop coefficients using leaf area index values, or incorporating a water stress coefficient could improve the equation's accuracy in comparison to direct eddy covariance evapotranspiration measurements. Measured average daily evapotranspiration ranged from 3.35 ± 1.70 (S.D.) mm day^{-1} (Miami) to 3.38 ± 1.78 mm day^{-1} (Glenlea). Most model adjustment combinations allowed cumulative evapotranspiration to be within 10% of measured cumulative evapotranspiration while the original FAO-56 equation estimated above the upper 10% error threshold at all locations. Growing season root mean square error and mean relative error values were lowest when all model improvements excluding the water stress coefficient were included. Improvements allow greater confidence in the FAO-56 Penman-Monteith equation's representation of canola evapotranspiration in Manitoba.

ACKNOWLEDGEMENTS

I'd like to thank the following individuals for their contribution and support throughout the entirety of this project:

Dr. Aaron Glenn and Dr. Brian Amiro, for the dedication of your time, patience and expertise as my advisors to ensure the success of this project and the growth of my knowledge as a scientist.

My committee members, Dr. Paul Bullock and Dr. Tim Papakyriakou, who offered their enthusiasm and advice for this project that helped motivate me throughout this process.

Clayton Jackson, as well as many summer students, for their incredible technical support throughout this project.

Dr. Sanjayan Satchithanantham, for your help with data processing and analysis, as well as your professional advice with writing and presenting.

Dr. Henry Wilson, for your advice throughout this project with writing and presenting.

To my many friends outside and within the Department of Soil Science who provided a wealth of support and encouragement. Specific requested shout-outs go to Chelsea, Kryssy, Liam, Rachel and Tyler.

To my family, especially my parents, who have devoted their time and energy to ensure I always found success. I am so privileged to be a part of this amazing family and could not imagine going through this project without you.

I would also like to thank Steppler Farms Ltd, CMCDC Carberry, and the University of Manitoba for providing land necessary for the completion of the project and for being incredibly cooperative.

Special thanks to the funding for this project provided by Growing Forward 2 and Research Manitoba. I am also incredibly grateful for scholarships provided by NorthStar Genetics Canada, Geza and Trudi Racz, Carl Shaykewich, and the University of Manitoba that helped financially support my studies.

TABLE OF CONTENTS

LIST OF TABLES

Table

LIST OF FIGURES

Figure

LIST OF ABBREVIATIONS

Abbreviation	
ET	Evapotranspiration
FAO	Food and Agriculture Organization
FAO-56	Food and Agriculture Organization Paper. 56
G	Ground Heat Flux
GDD	Growing Degree Days
H	Sensible Heat Flux
IRGA	Infra-red Gas Analyzer
K_c	Crop Coefficient
K_s	Stress Coefficient
LAI	Leaf Area Index
LE	Latent Heat Flux
LIDAR	Light Detection Ranging
MAWP	Manitoba Agriculture Weather Program
MRE	Mean Relative Error
NDAWN	North Dakota Agriculture Weather Program
PAM2nd	Prairie Agrometeorological Model
R_n	Net Radiation
RMSE	Root Mean Square Error
UV	Ultraviolet
u_*	Friction Velocity

1 INTRODUCTION

1.1 Overview

Evapotranspiration (ET) is the upward flux of water vapour from earth's surface to the atmosphere. It is considered the combination of evaporation and transpiration. Rates of ET are influenced by environmental factors like temperature, precipitation, wind speed, relative humidity and incoming solar radiation. But these rates are also influenced by the plants that inhabit the earth's surface and their ability to transpire. Trees, native grasses and agricultural crops all have different rates of transpiration throughout their life cycle that contribute to the total amount of ET from an ecosystem. Rates of transpiration increase from the point emergence occurs to vegetative maturity for argentine canola (*Brassica napus*). From vegetative maturity until pod ripening, transpiration rates plateau and then decrease when senescence begins. Total growing season ET for canola has varied over studies conducted on the Canadian prairies. Values reported include 353 mm in Carberry, MB (Martel et al., 2018), 264-286 mm in Saskatchewan (Cutforth et al., 2006), 250-450 mm across the Prairie Provinces (Cardillo, 2014) and 400-480 mm in Alberta (Alberta Agriculture and Forestry, 2013). By both understanding the pattern and the total losses of water vapour through ET, a producer can estimate how much water they are losing compared to how much they are gaining through precipitation/irrigation. This water balance could provide insight into potential yield limitations due to moisture stresses.

1.2 Importance of Canola (*Brassica napus*) in Canadian Crop Production

In the 2016 Census of Agriculture, there were 5839 farms across Canada that grew canola with a total area of 1,299,850 hectares (ha), which accounted for 15.5% of Canada's total agricultural land (Census of Agriculture, 2016). In 2018, Canada produced 20.3 million metric tonnes of canola. In 2017, Canada's total exports in canola were valued at $6.5 billion (Statistics

Canada, 2018). As global competition for oilseed production increases, it's important to ensure producers have highly productive canola crops.

A large contributor to high productivity in canola is adequate available water. Typically, the water demands of canola range from 0.1 mm day^{-1} of water at emergence to approximately 7 mm day^{-1} during periods of vegetative maturity in the average Canadian prairie climate (Alberta Agriculture and Forestry, 2011). The active root zone of canola reaches around 100 cm depth in a healthy, unimpeded soil with 70% of its water consumption coming from the top 50% of its active root zone (Alberta Agriculture and Forestry, 2011). These demands for water must be met to ensure high productivity from canola, but excessive moisture or irrigation can lead to yield limiting effects and impacts on the soil and surrounding environment.

Excessive moisture can lead to oxygen deficient soils, which decreases root development and impedes growth. Inappropriate irrigation or excessive precipitation can lead to run-off and leaching, carrying away valuable soil nutrients necessary for crop development. These nutrients (like phosphorus) carried in this water can further negatively impact aquatic ecosystems by fueling eutrophication, such as in Lake Winnipeg (Schindler et al., 2012). To be efficient with irrigation, it's important to apply when the crop needs it the most, and only apply to the crop demands. If at the start of the growing season the seed bed has a volumetric moisture content less than 60% of the available water holding capacity, 15 mm of irrigation should be applied as soon as irrigation water becomes available (Alberta Agriculture and Forestry, 2011). At this point, it's important to ensure a moist soil surface to prevent crusting, which limits emergence, but irrigation should be avoided if there is already a moist soil surface as additional irrigation can encourage soil crusting. Soil moisture after emergence should never fall below 60% of the available water holding capacity in the top 50 cm of the soil profile or it will inhibit aspects of plant, leaf, flower and seed development. With irrigation applications, soil depths between 50 and 100 cm should reach near field capacity to allow for adequate soil moisture when the root system is fully developed. At this point, there should be larger, less frequent irrigation events to ensure that the water is getting down farther in the root zone but also to limit the time canola is wet and susceptible to fungal diseases (Alberta Agriculture and Forestry, 2011).

1.3 Methods of Evapotranspiration Determination

Evapotranspiration can be determined using various methods, broadly sorted into measurement techniques and estimation techniques. Measurement techniques either look at the direct movement of water throughout the soil system and the atmosphere or the energy used for ET (latent heat flux). Examples of measurement techniques include the indirect energy budget and Bowen ratio methods, water balance methods including evaporation pans, the eddy covariance technique and large-scale evaporation measurements like light detection and ranging (LIDAR) measurements or scintillometer measurements (Shuttleworth, 2008). Estimation techniques are models that predict the amount of ET using meteorological variables that can contribute to ET like temperature, relative humidity, wind speed, and incoming solar radiation. Different types of estimation methods are Blaney-Criddle (1950), Makkink (1957), Turc (1961), Hamon (1963), Priestley-Taylor (1972), Hargreaves-Samani (1985), the FAO-56 Penman-Monteith equation (Allen et al., 1998) and Maulé et al (2006). The measurement technique focused on in this thesis was the eddy covariance technique. The eddy covariance technique determines the vertical fluxes of water vapour within the atmosphere to quantify surface water vapour losses. This method analyzes air for the direction it is moving, the speed at which it is moving and the concentration of water vapour held within the air (Burba & Anderson, 2010). This was done by using two main pieces of equipment, a sonic anemometer and a gas analyzer.

A sonic anemometer measures wind speed and direction by measuring the travel time of a sonic pulse between two transducers. These transducers are found on three planes so it can measure three-dimensional wind velocities. A gas analyzer determines the concentration of water vapour by measuring the amount of an emitted infrared or ultraviolet light source that is absorbed over a specific air sample. Since different gases absorb different frequencies of light, this information can be used to determine concentrations of gases by how much of a certain frequency of light is absorbed. The estimation technique considered in this thesis was the FAO-56 Penman-Monteith equation. This model uses four meteorological variables in its determination of ET (temperature, relative humidity, wind speed, and incoming solar radiation). Many other estimation techniques use three or less variables in their prediction of ET, but the FAO-56 Penman-Monteith method often follows the patterns of actual ET more closely compared to any other estimation technique (Allen et al., 1998). Even though it is considered the preferred method of ET estimation, there are still discrepancies between the FAO-56 Penman-Monteith and the eddy covariance ET measurements (Martel et al., 2018). These discrepancies suggest that the estimation technique has some issues with representing actual ET. In order for the FAO-56 Penman-Monteith equation to be used with greater confidence in representing actual ET, improvements to the model's generation of ET should be examined.

1.4 Minimizing Differences between Eddy Covariance and the FAO-56 Penman-Monteith equation

There are three potential methods of minimizing the discrepancies in ET between the eddy covariance technique and the FAO-56 Penman-Monteith equation proposed in this thesis. The three include: (1) incorporating directly measured available energy (net radiation – ground heat flux), (2) creating a dynamic crop coefficient more representative of the specific agroecosystem with weekly leaf area index (LAI) measurements, and (3) incorporating a water stress coefficient into the equation.

By incorporating directly measured available energy instead of estimated net radiation and ground heat flux, the estimated ET should theoretically have fewer discrepancies when compared to measured ET. It was surmised that including measured values in a model rather than values that would be normally estimated, the model should represent measured ET more accurately as there are fewer components that need to be estimated. Determining available energy can be done using net radiometers to measure net radiation and ground heat flux can be determined by measuring the heat flux at a fixed depth using soil heat flux plates and adding it to the stored energy in the soil above this depth.

Crop coefficients are values used to translate reference ET generated by the FAO-56 Penman-Monteith equation for a particular reference crop to actual ET for any crop of interest. Standard crop coefficients have been developed with three different values to represent the development of the crop. For example, the initial crop coefficient for canola is 0.35, the mid-season crop coefficient is 1.15 and the end crop coefficient is 0.35 (Allen et al., 1998). These values are held constant irrespective of canola variety, plant density, or any other variables besides plant species. Even between fields with the same crop species, agroecosystems are diverse and develop differently throughout growing seasons and locations, so having a 3-point crop coefficient might be where discrepancies originate between measured and modelled ET. Leaf area index measured on a weekly basis reflects the development of plant biomass throughout the growing season. A time series of leaf area index values throughout the growing season can create a trend that can be translated to a crop coefficient pattern that is more representative of biomass development in the field, and create a more accurate estimate of actual ET.

The final method of improvement to the model is through the incorporation of a water stress coefficient. Stresses due to excess and deficient available water in the soil for plant consumption lead to decreased rates of ET. These stresses are not accounted for in the basic FAO-56 Penman-Monteith equation and therefore if the agroecosystem is stressed, the model will not be able to represent actual ET accurately. This stress can be determined by the total available water, the readily available water and the depletion rate of this water. These values are generated using field capacity and permanent wilting point of the soil system, assumed rooting depth of the crop, depletion factor unique to the crop generated by the FAO, inputs of precipitation and irrigation, rates of ET, and a single value of soil moisture content at the start of the growing season.

1.5 Study Objectives

The first objective of the project was to calculate the differences in estimated ET generated from the FAO-56 Penman-Monteith equation, crop coefficients generated from the FAO for canola, and water stress coefficients compared to measured ET values through eddy covariance over three fields of canola across southern Manitoba. By noting the differences and similarities between estimating and measuring ET, the estimation method can either be further validated or it could lead to further research on how to make the estimation method more accurate for that agroecosystem.

A second objective of this project was to minimize the differences between estimated ET through the FAO-56 Penman-Monteith equation and measured ET through the eddy covariance method. Possible ways to minimize the difference were to incorporate measured net radiation and ground heat flux into the FAO-56 Penman-Monteith equation, generate field specific crop coefficients using LAI, and applying a water stress coefficient generated by the FAO to characterize soil moisture.

A third objective of this project was to complete a comparison between in-field reference ET and regional estimates from the Manitoba Ag-Weather Program (MAWP).

1.6 References

Alberta Agriculture and Forestry. 2011. Irrigation scheduling for canola in Southern Alberta. URL https://www1.agric.gov.ab.ca/$department/deptdocs.nsf/all/agdex13575.

Alberta Agriculture and Forestry. 2013. Alberta irrigation management manual. URL https://www1.agric.gov.ab.ca/$department/deptdocs.nsf/all/irr14310.

Allen, R. G., Pereira, L. S., Raes, D., & Smith, M. 1998. Crop evapotranspiration-guidelines for computing crop water requirements. FAO Irrigation and Drainage Paper No. 56, FAO, Rome, Italy. URL http://www.fao.org/3/X0490E/x0490e00.htm#Contents.

Blaney, H.F., & Criddle, W.D. 1950. Determining water requirements in irrigated areas from climatological and irrigation data. Soil Conservation Service Technical Paper 96. Soil Conservation Service. U.S. Department of Agriculture, Washington, USA.

Burba, G., & Anderson, D. 2010. A brief practical guide to eddy covariance flux measurements: principles and workflow examples for scientific and industrial applications. Li-Cor Biosciences.

Cardillo, M. J. 2014. Stubble management effects on microclimate and performance of canola across different climatic regions in Western Canada. M.Sc. Thesis. University of Manitoba.

Census of Agriculture. 2016. Hay and field crops. URL https://www150.statcan.gc.ca/t1/tbl1/en/tv.action?pid=3210041601.

Cutforth, H. W., Angadi, S. V., & McConkey, B. G. 2006. Stubble management and microclimate, yield and water use efficiency of canola grown in the semiarid Canadian Prairie. *Can. J. Plant Sci.*, ***86***(1), 99-107.

Hamon, W. R. 1963. Computation of direct runoff amounts from storm rainfall. *Int. Assoc. Sci. Hydro. Pub.*, ***63***, 52-62.

Hargreaves, G. H., & Samani, Z. A. 1985. Reference crop evapotranspiration from temperature. *Appl. Eng. Agric.*, ***1***(2), 96-99.

Makkink, G. F. 1957. Testing the Penman formula by means of lysimeters. *J. Inst. Water Eng.*, ***11***, 277-288.

Martel, M., Glenn, A., Wilson, H., & Kröbel, R. 2018. Simulation of actual evapotranspiration from agricultural landscapes in the Canadian Prairies. *J. Hydro: Regional Studies.*, ***15***, 105-118.

Maulé, C., Helgason, W., McGinn, S., & Cutforth, H. 2006. Estimation of standardized reference evapotranspiration on the Canadian Prairies using simple models with limited weather data. *Can. Biosystems Eng.*, ***48***, 1.1-1.11.

Priestley, C. H. B., & Taylor, R. J. 1972. On the assessment of surface heat flux and evaporation using large-scale parameters. *Mon. Weather Rev.*, ***100***(2), 81-92.

Schindler, D. W., Hecky, R. E., & McCullough, G. K. 2012. The rapid eutrophication of Lake Winnipeg: Greening under global change. *J. Great Lakes Res.*, ***38***, 6-13.

Shuttleworth, W. J. 2008. Evapotranspiration measurement methods. *SW. Hydro.*, ***7***(1), 22-23.

Statistics Canada. 2018. Fields of gold: Canola exports and production. URL https://www150.statcan.gc.ca/n1/pub/11-627-m/11-627-m2018044-eng.htm.

Turc, L. 1961. Water requirements assessment of irrigation, potential evapotranspiration: simplified and updated climatic formula. *Ann. Agron.*, ***12***, 13-49.

2 DETERMINING EVAPOTRANSPIRATION AND CROP COEFFICIENT VALUES USING AN ADJUSTED PENMAN-MONTEITH EQUATION OVER CANOLA (*Brassica napus*) IN SOUTHERN MANITOBA.

2.1 Abstract

The FAO-56 Penman-Monteith equation and crop coefficients were adjusted to better represent modern canola (*Brassica napus*) grown in Manitoba at three locations. It was hypothesized that incorporating direct measurements of available energy, developing crop coefficients using leaf area index values, or incorporating a water stress coefficient could improve the equation's accuracy in comparison to direct eddy covariance evapotranspiration measurements. Measured average daily evapotranspiration ranged from 3.35 ± 1.70 (S.D.) mm day^{-1} (Miami) to 3.38 ± 1.78 mm day^{-1} (Glenlea). Most model adjustment combinations allowed cumulative evapotranspiration to be within 10% of measured cumulative evapotranspiration while the original FAO-56 equation estimated above the upper 10% error threshold at all locations. Growing season root mean square error and mean relative error values were lowest when all model improvements excluding the water stress coefficient were included. Improvements allow greater confidence in the FAO-56 Penman-Monteith equation's representation of canola evapotranspiration in Manitoba.

2.2 Introduction

Evapotranspiration (ET), and the rate it is produced in an agroecosystem, is a vital component in the understanding of water movement in agricultural fields. The majority of water removed from the soil system on the Canadian prairies throughout the growing season is through ET, so being able to quantify these values can give insight as to available moisture for plant uptake (Fang et al., 2007). Measurement techniques like the eddy covariance method can be used to determine the rates of ET, but require instrumentation that can be costly (Burba and Anderson, 2010). Estimation techniques like the FAO-56 Penman-Monteith equation use meteorological data gathered at most weather stations across Manitoba to determine actual ET (Allen et al., 1998). As these data are more available for most agricultural locations across the province, this estimation technique could be used, as long as it represents ET accurately. Although the FAO-56 Penman-Monteith equation is considered the preferred method of ET estimation, there are still discrepancies compared to direct measurements of ET (Martel et al., 2018). As the eddy covariance technique is a direct measurement of fluxes of water vapour leaving the field system, any discrepancies with the estimation technique would mean problems with the FAO-56 Penman-Monteith equation's representation of actual ET.

Multiple field comparisons of the FAO-56 Penman-Monteith equation and eddy covariance generated ET for argentine canola have not been done in southern Manitoba. As the crop coefficient value for the FAO-56 Penman-Monteith equation has been generated for canola/rapeseed grown in the central United States during the late 1990s, it's important to ensure that the model represents canola that is currently grown in southern Manitoba as well (Allen et al., 1998). Comparing measured and estimated ET over multiple sites of canola in Manitoba will produce knowledge about uncertainties and potential biases.

Certain adjustments to the model can be done to potentially improve the method including incorporating direct measurements of available energy, generating a dynamic crop coefficient from LAI measurements and by incorporating a water stress coefficient. If these improvement methods help minimize discrepancies between estimated and measured ET, and create more representative values of actual ET over a field of canola, the FAO-56 Penman-Monteith equation can be used with greater confidence to represent actual ET across southern Manitoba and help map the movement of water throughout various agroecosystems.

2.3 Study Objectives

The first objective of the project was to measure the differences in estimated ET generated from the FAO-56 Penman-Monteith equation, crop coefficients generated from the FAO for canola, and water stress coefficients compared to measured ET values through eddy covariance over three fields of canola across southern Manitoba. By noting the differences and similarities between estimating and measuring ET, the estimation method can either be further validated or it could lead to further research on how to make the estimation method more accurate for that agroecosystem.

A second objective of this project was to minimize the differences between estimated ET through the FAO-56 Penman-Monteith equation and measured ET through the eddy covariance method. Possible ways to minimize the difference were to incorporate measured net radiation and ground heat flux into the FAO-56 Penman-Monteith equation, generate field specific crop coefficients using LAI, and applying a water stress coefficient generated from the FAO to represent soil moisture.

A third objective of this project was to complete a comparison between in-field reference ET and regional estimates from the Manitoba Ag-Weather Program (MAWP).

2.4 Hypothesis

It was hypothesized that there would be apparent differences between measured and modelled ET at all sites, and that the incorporation of measured available energy, a dynamic K_c using LAI, and a water stress coefficient would improve the agreement between measured and modelled ET. It was also hypothesized that comparisons between reference ET generated using weather data collected in-crop and on the intended grass surface through MAWP within 1 km of each other will have minimal differences.

2.5 Methods

2.5.1 Site Description

Three locations across southern Manitoba were used in this experiment. The first field was on the Canada Manitoba Crop Diversification Centre farmland 2 km north of Carberry, MB 49. 91°N, 99. 35°W). The second field was located on Steppler Farms Ltd. land west of Miami, MB alongside South Tobacco Creek (49. 34°N, 98. 37°W). The third field was on the University of Manitoba's Trace Gas Manitoba Greenhouse Gas Field Emission Site close to Glenlea, MB, which was 15 km south of Winnipeg, MB (49. 65°N, 97. 16°W). The field sizes were 12.8 ha at Carberry, 16.0 ha at Miami and 47.6 ha at Glenlea. The three sites are within 160 km of each other and reside in a cool, humid continental climate as classified by the Köppen climate classification system. Moisture inputs at Carberry were greater than at Glenlea and Miami, but this was due to the implementation of irrigation and not due to differences in weather. Each site grew canola for the 2018 growing season, but each had slight differences in their agroecosystem as mentioned in Table 2.1. Differences in previous crop, soil type, variety, and harvest method can lead to differences in yield.

Table 2.1 Land and crop characteristics for the 2018 growing season at three locations.

	Carberry	**Miami**	**Glenlea**
Location	SE 8-11-14-W	NE 29-4-7-W	NORL 6,7,8
Canola Variety	Invigor L252	Invigor L252	Invigor L233P
Previous Crop	Spring Wheat (*Triticum aestivum*)	Soybeans (*Glycine max*)	Maize (*Zea mays*)
Soil Type	80% Ramada Series (RAM) (Class 1) 20% Wellwood Series (WWD) (Class 1)	100% Dezwood Series (DZW) (Class 2T)	70% Red River Series (RIV) (Class 2W) 30% Osborne Series (OBO) (Class 3W)
Maximum Crop Height (m)	1.11	0.89	0.94
Final Plant Density (plants m^{-2})	40.1	21.4	24.9
Harvest Method	Straight Cut	Swathed	Straight Cut
Aboveground Biomass (kg ha^{-1})	7204	5746	5042
Grain yield (kg ha^{-1})	2825	2358	1396

2.5.2 Measurement Methods

2.5.2.1 Direct Evapotranspiration Measurements. At all three sites, measurements of ET were obtained through the eddy covariance method. Each location used slightly different equipment to determine ET. At Carberry, the site had a LI-7200 enclosed-path infra-red gas analyzer (IRGA) (LI-7200, LI-COR Inc., Lincoln, NE, USA) and a 3-D sonic anemometer (model CSAT3, Campbell Sci., Logan, UT, USA). Miami had a combined sonic anemometer and open-path infra-red gas analyzer (IRGASON, Campbell Sci., Logan, UT, USA). At Glenlea, the site had a krypton hygrometer (model KH20, Campbell Sci., Logan, UT, USA) and a 3-D soil anemometer (model CSAT3, Campbell Sci., Logan, UT, USA).

For Carberry and Miami, the initial intake heights of the IRGAs and sonic anemometers were set to a height of 2 m above the soil surface. At the point in the growing season where some of the canola plants were above 1 m in height, the IRGAs and sonic anemometers were raised to 2.25 m. The IRGAs and sonic anemometers were returned to a height of 2 m after harvest was completed. At Glenlea, the hygrometer and sonic anemometer remained at 2.5 m the whole growing season. At all three sites, the gas analyzers and sonic anemometers were set directly west. Distance between the gas analyzer and the sonic anemometer was set to 13 cm at Carberry and Glenlea.

Lab calibration of the IRGAs water vapour channels were done after harvest (fall 2017) and right before seeding (spring 2018). A zero gas was used (0ppt of water vapour) and a specified concentration of water vapour to have a dew point of 20°C generated by a dew point generator. Throughout the growing season, if the IRGA was suspected to have drifted in its accuracy of measurement, an in-field zero calibration with a zero gas was done. This happened once at Miami (July 18th) and once at Carberry (July 27th). Maintenance of equipment was mainly the cleaning of optic windows, which was done whenever the signal strength was below 90%. For calibrating the sonic anemometer, a bag test was done either in-lab or in-field to check for zero velocities. The KH20 was sent for a factory calibration over the winter of 2017-2018. Other general maintenance was done like removal of animal and plant debris from these sensors when it could block or interfere with measurements.

2.5.2.2 Supporting Environmental Measurements. Additional meteorological measurements were made at each site for inputs to the FAO-56 Penman-Monteith equation. A temperature/humidity sensor with a radiation shield (HMP 155, Campbell Scientific, Logan, UT, USA) was set to a height of 1.5 m and was used at each site for ambient temperature values and relative humidity. Net radiometers (NR Lite 2, Kipp & Zonen, Rotterdam, The Netherlands) were used to measure net radiation, which is necessary for the adjustment to the model of measured available energy in the model. Two net radiometers were used at Miami and Carberry and one was used at Glenlea. They were installed at a height of 1.5 m. Soil heat flux plates

(HTF3, Campbell Scientific, Logan, UT, USA) were used at each site to characterize the soil heat flux, a component in the adjustment of using measured available energy. They were installed parallel to the soil surface at 8-cm depth. Soil temperature and moisture sensors (5TM, Meter Group Inc., Pullman, WA, USA) determined soil moisture content within the initial depths of soil and were inserted parallel to the soil surface at 5-cm depth. This information was used to generate the soil temperature correction for the soil layer above the soil heat flux plates. Precipitation was determined using a tipping bucket set at a height of 1 m (TR252, Texas Instruments, Dallas, TX, USA). There were secondary microclimate stations that included temperature/relative humidity sensors (ATMOS 14, Meter Group Inc., Pullman, WA, USA) at a height of 1.5 m, solar radiation sensors (PYR, Meter Group Inc., Pullman, WA, USA) at a height of 1.5 m, cup anemometers (Davis, Meter Group Inc., Pullman, WA, USA) at a height of 2 m, and tipping buckets (ERHN 100, Meter Group Inc., Pullman, WA, USA) at a height of 2 m. There were additionally lysimeters (Drain Gauge G2, Meter Group Inc., Pullman, WA, USA) that were used to help determine soil moisture at certain depths (20 cm, 50 cm and 100 cm). Lysimeter data at the 20 cm depth were used to help create a water stress coefficient by generating an initial volumetric water content based on lysimeter data measured at seeding, which was one of the criteria needed to generate the water stress coefficient.

Crop-height, crop-staging and leaf area index values were taken on a weekly basis at each site. Twenty crop-height measurements were taken and the median was recorded as the height for that day. Five measurements were taken in each direction (N, S, E, and W) with each measurement being 5, 10, 15, 20, and 25 m away from the eddy covariance flux tower. Crop-staging was done by using the Canola Council of Canada crop-staging guide in all four directions from the eddy covariance tower. Pictures were taken along with trail camera (BirdCam Pro, Wingscapes, Calera, AL) pictures 4 times a day (9am, 12pm, 3pm, and 6pm) to confirm correct assessments of crop development out of field. LAI values were taken using a LAI-2200 (LI-COR Inc., Lincoln, NE) on a weekly basis. There were 20 samples of LAI taken per site visit in the same positions as the 20 crop-height measurements. Each sample included one above-canopy measurement and four below-canopy measurements spaced 5 cm apart. There were also four initial above-canopy measurements used to develop a scattering correction. These four measurements were as follows: one with an opaque diffuser cap in the sun, one with the diffuser cap shaded, one with no cap shaded, and one with the normal view cap pointing in the sampling direction. Each direction (N, S, E, and W) generated one value of LAI so there were four values of LAI for each location every week. LAI measurements were also graded using the rating system in Table 2.2 to signify if the measurements were taken at an ideal time. If the conditions were too poor (≤ 1), LAI measurements were not collected. Leaf area index values were removed from the data if their scattering correction was greater than 1 or if there was reason to believe that the crop stand was not representative of the entire field.

Table 2.2 Sky and weather conditions to signify the quality of LAI data being collected.

Rating	Sky/Weather Conditions
3	Clear sky, dusk or dawn
2	Uniform sky conditions, not directly mid-day (perfectly sunny or uniformly cloudy and before noon or after 2)
1	Uneven cloud coverage or directly mid-day (12-1)
0	Rainy and windy in addition to uneven clouds

Aboveground biomass was determined using a similar sampling pattern as was done for LAI measurements. Samples were taken N, S, E, and W of the eddy covariance flux station. Instead of five samples 5 m apart in each direction, aboveground biomass sampling was three samples 10 m apart in each direction (n=12). This gave four samples 10 m away from the eddy covariance flux station, four samples 20 m away, and four samples 30 m away. Each sample was one-metre-long row of canola.

Seed yield was determined by the dry weight of seed biomass sampled within a week of the crop being harvested. This value was then determined in kg ha^{-1} calculated from grams of seed weighed and the area measured at each site based on row spacing for each field. The area was determined by 12 samples of 1 m row taken with the method stated previously in Section 2.5.2.1 and using the row spacing to determine how many rows would exist in 1 m^2. This value was then used to determine the area needed to encapsulate 12 meter-long rows. Row spacing for the canola at Carberry and Miami was 26.7 cm, with 3.75 rows of canola in m^2 sample, giving 12 samples in 3.2 m^2. Canola grown in Glenlea had a row spacing of 38.1 cm, with 2.62 rows of canola in a m^2 sample and ultimately led to 12 samples to be in 4.58 m^2.

Stand density measurements were taken by counting the number of plants in a row along one meter at the same points where the aboveground biomass was taken. Samples were translated to m^2 samples of plant density by accounting for the row spacing (26.7 cm at Carberry and Miami, 38.1 cm at Glenlea), totalling the amount of canola plants in the 12 meter-long samples, and then dividing that total density by the area needed to encapsulate 12 meter-long samples (3.2 m^2 for Carberry and Miami and 4.58 m^2 for Glenlea).

2.5.3 Data Processing

2.5.3.1 Eddy Covariance Measurements. Raw output from the gas analyzers and sonic anemometers was recorded by a data logger (model CR3000, Campbell Sci., Logan, UT) at Miami and Glenlea. The frequency of raw data in the case of Miami and Glenlea was 10 Hz. At Carberry, raw data were collected at a frequency of 20 Hz, using a different data logger (model LI-7550, LI-COR Inc., Lincoln, NE). These raw data were then processed and filtered in

EddyPro v6.2.1 software (LI-COR Inc., 2017). Spike deviations (>3.5 standard deviations) from the mean for H_2O concentration and wind velocity components over 5-minute time windows were removed and filled by linear interpolation (Vickers and Mahrt, 1997). If more than 3 consecutive outliers existed for a value, they were not removed as it could potentially be a sign of an unusual physical trend. The coordinate rotation used was double rotation, which means that the raw wind components were to set the mean vertical velocity ($\overline{w}$) to zero, and then rotated so that the mean u was along the direction of the mean wind. All the high frequency raw data were then processed into 30-minute block average values of sensible and latent heat fluxes. For all sites, spectral correction factors were applied to fluxes in both the low (Moncrieff et al. 2004) and high frequency (Moncrieff et al. 1997) range to address high-pass and low-pass filtering effects, respectively. The Moncrieff et al. approaches are purely analytical as flux attenuation caused by instrument set-up, detrending method, and flux spectral properties are modelled using mathematical formulation and corrected with transfer functions. Plausibility limits were set to remove unrealistic 30-minute latent heat, sensible heat and H_2O fluxes. Anything outside of -200 to 1000 W m^{-2} for latent heat and sensible heat fluxes were removed. H_2O fluxes outside -2 and 30 mm and H_2O mixing ratios outside 0 to 50 mmol mol^{-1} were removed as well.

After the data were processed through EddyPro, it was filtered with a method proposed by Papale et al. (2006) using R (R Core Team, 2018) to detect and remove outlier data in water vapour fluxes. This filter used median absolute deviation, which is a robust outlier estimator. A spike threshold (z) of 4 was used which is most conventionally used and is the least conservative method of filtering (Papale et al., 2006).

Clean data were then exported as csv files to be used by Matlab R2013b software (Mathworks, 2013) for further processing. Quality control flags of 2 that are assigned by

EddyPro (Mauder and Foken, 2011) were removed from the data set. A value of 2 suggests the data are of the lowest quality and should not be used to represent distinct fluxes and flux patterns. A friction velocity (u_*) threshold of less than 0.1 m s^{-1} was set to remove data where there was insufficient turbulence to measure fluxes. Before any gap-filling procedures started, energy balance closure was forced. The energy balance closure procedure took 30-minute data points where no gaps in the energy balance components (net radiation, latent heat flux, sensible heat flux and ground heat flux) existed, these values were totalled for the growing season and the available energy (R_n – G) were divided by the combination of latent and sensible heat. This generated a multiplier that was applied to latent and sensible heat fluxes on a 30-minute basis. Any gaps in net radiation, latent heat flux, sensible heat flux and ground heat flux were either filled using linear interpolation (gaps < 2 hours) or a regression-based gap-filling method for longer gaps (Barr et al., 2004). This gap-filling method separates daytime and nighttime data, and utilizes regression coefficients of energy fluxes to fill gaps using a moving-window approach where fits of 240 observations at a time were solved with incremental changes of 48 points for a half-hour dataset. The calculated average 90% footprint at each site was 331 m at Carberry, 407 m at Miami, and 516 m at Glenlea.

Random error values were assigned to LE associated with the eddy covariance technique by EddyPro v6.2.1 software (LI-COR Inc., 2017) using a cross-correlation function that uses the calculation of "variance of covariance" (Finkelstein and Sims, 2001). These error values were used to validate error thresholds around cumulative measured ET.

2.5.3.2 Penman-Monteith Modelling. Gaps in temperature, relative humidity, wind speed, incoming solar radiation and precipitation were filled using secondary weather data collected at the sites. Linear regression between primary and secondary sourced data were used for gap-filling.

The FAO-56 Penman-Monteith equation's (Eq. 1) reference ET data were generated in Excel (Microsoft, 2016) using inputs of temperature, relative humidity, wind speed and solar radiation. FAO crop coefficients were applied to the reference ET using crop staging at each site (initial K_c at emergence, mid K_c at inflorescence emergence, and end K_c at senescence) to translate ET for a reference surface to ET that is actually representative of the canola (Eq. 2). Values were taken directly from Table 12 in the FAO report on the Penman-Monteith equation titled "Single (time-averaged) crop coefficients, K_c, and mean maximum plant heights for non stressed, well-managed crops in subhumid climates (RHmin » 45%, u_2 » 2 m s^{-1}) for use with the FAO Penman-Monteith ETo" for canola (rapeseed) (Allen et al., 1998). Direct measurements of net radiation and ground heat flux were input into the FAO-56 Penman-Monteith equation (Eq. 1) through Excel as part of the first improvement of the model.

$$ET_{ref} = \frac{0.408\Delta(R_n - G) + \gamma\frac{900}{T+273}u_2(e_s - e_a)}{\Delta + \gamma(1 + 0.34u_2)} \text{ (Eq. 1)}$$

Where ET_{ref} is reference evapotranspiration [mm day^{-1}], R_n is net radiation at the crop surface [MJ m^{-2} day^{-1}], G is soil heat flux density [MJ m^{-2} day^{-1}], T is mean daily air temperature at 2 m height [°C], u_2 is wind speed at 2 m height [m s^{-1}], e_s is saturation vapour pressure [kPa] at temperature T, e_a is actual vapour pressure [kPa], Δ is the slope of the vapour pressure curve [kPa $°C^{-1}$], and γ is psychrometric constant [kPa $°C^{-1}$] (Allen et al., 1998).

$$ET_a = ET_{ref} \times K_c \times K_s \text{ (Eq.2)}$$

Where ET_a is actual evapotranspiration [mm day^{-1}], ET_{ref} is reference evapotranspiration [mm day^{-1}], K_c is the crop coefficient, and K_s is the stress coefficient (Allen et al., 1998). The K_s is only necessary to apply during periods of suspected drought stress.

After low-quality LAI data were removed, average LAI for each day was generated using the 4 LAI samples that were taken around each flux tower. Crop coefficients were calculated using a 3rd order polynomial equation created to fit these averages and then the curve was fitted so that the highest point in the equation would be 1.15, the mid-season crop coefficient for canola from the FAO-56 Penman-Monteith equation. This crop coefficient was then multiplied by the unaltered reference ET generated by the FAO-56 Penman-Monteith equation to get another improvement method for the model.

Water stress coefficients were generated through Excel using the procedure outlined in the paper including the FAO-56 Penman-Monteith equation (Allen et al., 1998). The procedure required values of rooting depth, field capacity, permanent wilting point, volumetric moisture content and precipitation. Rooting depth was estimated using a crop staging guide created by the Canola Council of Canada that estimated rooting depth using days after seeding (Canola Council of Canada, 2016). Field capacity and permanent wilting point were taken from the Government of Canada's CanSIS Soils of Manitoba database (Government of Canada, 2013).

Growing degree days (GDD) were determined using temperature data to help compare the phenological staging done at the three sites:

$$\mathrm{GDD} = \frac{\mathrm{T_{max}} + \mathrm{T_{min}}}{2} - \mathrm{T_b} \text{ (Eq. 3)}$$

Where GDD is the growing degree days, T_{max} is the daily maximum temperature (°C), T_{min} is the daily minimum temperature (°C), and T_b is the base temperature (°C) which is set to 5°C.

Regional reference ET over a grassed surface was determined by applying values of temperature, relative humidity, wind speed and solar radiation collected from the Manitoba Agriculture Weather Program (MAWP) weather station located less than one kilometre west of our micrometeorology/flux station north of Carberry, MB. This MAWP weather station was maintained over a short grass reference surface assumed with values of 0.12 m crop height, 70 s m^{-1} surface resistance, and 0.23 albedo input into the FAO-56 Penman-Monteith equation as a regional estimate.

2.5.4 The FAO-56 Penman-Monteith Equation

The FAO-56 Penman-Monteith equation is one of the most commonly used ET models. It’s considered one of the best methods of determining ET compared to measured techniques, but there are still discrepancies from this model when compared to measured ET.

As mentioned previously, there are 4 inputs for the model, maximum and minimum daily temperature, maximum and minimum daily relative humidity, average daily wind speed and total daily incoming solar radiation. Relative humidity was used to generate saturation vapour pressure and actual vapour pressure. Incoming solar radiation was used to estimate values of net radiation. Values of temperature were used to determine values of mean saturation vapour pressure and actual vapour pressure, as well as, directly in the equation. Wind speed was used directly in the equation as well.

The FAO-56 Penman-Monteith equation itself was used as a baseline for proposed improvements. The proposed improvements are listed as follows:

1. Using direct measurements of available energy

The first proposed improvement was simple in the adjustments to the FAO-56 Penman-Monteith equation. The incorporation of net radiation (R_n) and ground heat flux (G) taken by the net radiometer and soil heat flux plates were directly used in the FAO-56 Penman-Monteith equation, instead of estimated from incoming solar radiation. This would improve the reference ET estimation.

2. Using LAI measurements to generate daily crop coefficient values

The second model improvement does not affect the FAO-56 Penman-Monteith determination of reference ET, but changes the crop coefficient that is used to translate the reference ET to actual ET for the crop of canola. Leaf area index values that were measured weekly were filtered and averaged to create a LAI value that represents the canola for each day. Using these points of LAI, a 3rd order polynomial curve was fit to represent the dynamic changes in LAI from emergence to harvest. Leaf area index points that laid directly on the crest of the curve were deemed the max crop coefficient value for canola of 1.15 and then the rest of the LAI values were scaled down for K_c. Any period deemed phenologically in the initial and end crop coefficient stages was given a fixed value of 0.35.

To make the equation represent LAI of the canola when measurements were not possible, an estimation of LAI was added at the crop stage when K_c initial was determined to be overestimated by the FAO. This estimation technique was taken from the FAO-56 Penman-Monteith equation paper and determines active plant biomass by crop height (Allen et al., 1998). With estimated crop height at this stage, it was translated to estimated LAI, which was incorporated into the polynomial equation which helped represent ET when the plants were developing plant biomass, but still not the right size to measure LAI accurately.

3. Incorporating a water stress coefficient generated from soil moisture data

The third model improvement required information about the rooting depth, field capacity, permanent wilting point, average volumetric moisture content, ET and precipitation. These are used to derive the water stress coefficient for FAO-56 Penman-Monteith (Allen et al., 1998). We first calculated TAW, which is the total available soil water in the root zone:

$$\mathrm{TAW} = 1000(\theta_{\mathrm{FC}} - \theta_{\mathrm{WP}})\, Z_r \text{ (Eq. 4)}$$

Where TAW is the total available soil water in the root zone [mm], θ_{FC} is the volumetric water content at field capacity [m^3 m^{-3}], θ_{WP} is the volumetric water content at the wilting point [m^3 m^{-3}], and Z_r is the rooting depth [m].

Next, we calculate RAW, which is the readily available soil water in the root zone:

$$\mathrm{RAW} = p\ \mathrm{TAW} \text{ (Eq. 5)}$$

Where RAW is the readily available soil water in the root zone [mm], and p is the average fraction of Total Available Soil Water (TAW) that can be depleted from the root zone before moisture stress (reduction in ET) occurs [0.6 for canola] (Allen et al., 1998).

The $D_{r,\,i}$, or the root zone depletion at the end of the day i is calculated through a water balance as:

$$D_{r,i} = D_{r,i-1} - (P - RO)_i - I_i - CR_i + ET_{c,i} + DP_i \text{ (Eq. 6)}$$

Where $D_{r,\,i}$ is the root zone depletion at the end of day i [mm], $D_{r,\,i\text{-}1}$ is the water content in the root zone at the end of the previous day, i-1 [mm], P_i is the precipitation on day i [mm], RO_i is the runoff from the soil surface on day i [mm], I_i is the net irrigation depth on day i that infiltrates the soil [mm], CR_i is the capillary rise from the groundwater table on day i [mm], $ET_{c,\,i}$ is the crop evapotranspiration on day i [mm], and DP_i is the water loss out of the root zone by deep percolation on day i [mm].

For Equation 6, values of run-off, capillary rise and deep percolation were assumed to be zero, and for Miami and Glenlea, irrigation was assumed to be zero. Crop ET for this equation is suggested to be determined by the FAO-56 Penman-Monteith equation, but as eddy covariance measurements of ET at the sites were available, these values of ET were used instead.

In order to generate a value for initial water content in the root zone, the following equation was used. The only new input is the use of $\theta_{i\text{-}1}$, the average volumetric water content in the soil [$m^3\ m^{-3}$], which was the first data point collected using the G2 lysimeter at the 20 cm depth at the start of the growing season.

$$D_{r,i-1} = 1000(\theta_{FC} - \theta_{\,i-1})\, Z_r \text{ (Eq. 7)}$$

If the root zone depletion is greater than the readily available water, then K_s is:

$$K_s = \frac{TAW - D_r}{TAW - RAW} = \frac{TAW - D_r}{(1-p)TAW} \text{ (Eq. 8)}$$

where K_s is a dimensionless transpiration reduction factor dependent on available soil water [0 - 1].

A typical water stress coefficient ranges from 0 [maximum water stress] to 1 [no water stress], but a minimum crop stress coefficient of 0.1 is used, as 0 suggests no ET at all and it is unrealistic that there will ever be a period with no ET during the growing season (Alberta Agriculture and Forestry, 2013).

2.5.5 Statistical Analysis

Each modelled value of daily ET was compared to the measured ET with an ordinary least squares linear regression where measured ET was the independent variable. These modelled values include the model with each improvement and every possible combination of improvements. The coefficient of determination (R^2) were used for comparisons of daily estimated ET to daily measured ET. Root mean square error (RMSE) and mean relative error (MRE) were also used to compare daily agreement between estimated and measured daily ET. The R^2, RMSE and MRE were calculated using methods outlined in Martel et al. (2018). Cumulative ET was compared for every combination of model improvements throughout the growing season. Error lines of 10% above and below the measured ET based on random error assigned for LE calculated using the eddy covariance method were set to show uncertainty in estimated cumulative ET throughout the growing season.

2.6 Results

2.6.1 Growing Season Evapotranspiration and Weather Conditions

Measured ET throughout the growing season at all three sites was similar. Carberry had the greatest amount of ET with 337 mm over a 100-day growing season (3.37 mm day^{-1}). Glenlea had the least with 328 mm of ET over a 97-day growing season (3.38 mm day^{-1}). Miami had 332 mm of ET over a 99-day growing season (3.35 mm day^{-1}). The pattern of ET was similar for all three sites and followed what was expected for an annual cropping system (Figure 2.1).

Peak rates of ET occurred in the middle of the growing season, approximately between day 185 and 200, when the crop had reached vegetative maturity.

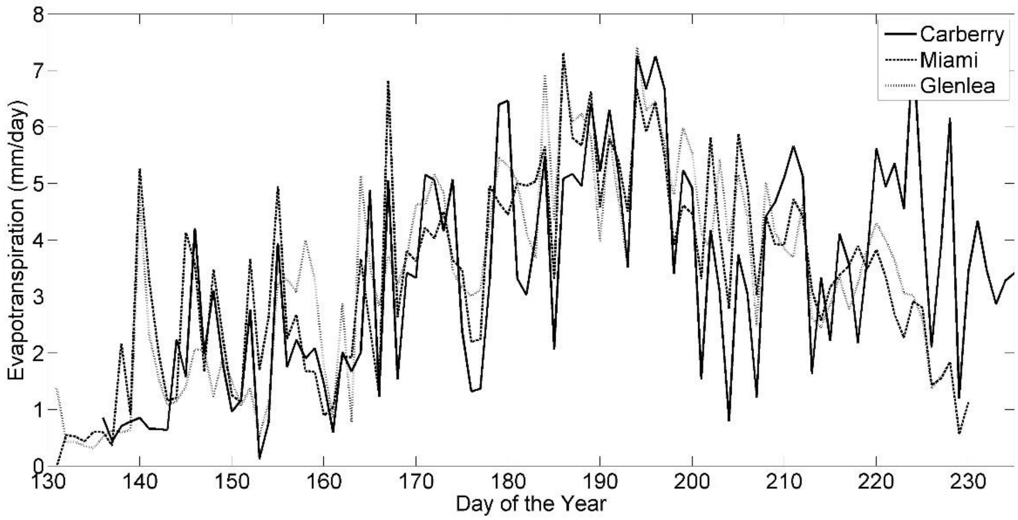

Figure 2.1 Daily measured ET values for 3 sites (Carberry, Miami, and Glenlea) of canola (*Brassica napus*) over the 2018 growing season.

For measured ET, the sample sizes of 30-minute latent heat flux data points for the 3 sites after data cleaning and before gap filling were n=3812 (Carberry), n=3913 (Miami), n=2646 (Glenlea). After gap-filling was done, the sample sizes were n=4800 (Carberry), n=4752 (Miami), and n=4656 (Glenlea). This means that 21% of Carberry's data for the latent heat flux were gap-filled, 18% of Miami's data were gap-filled, and 43% of Glenlea's data were gap-filled.

Weather data for all three sites were relatively similar (Table 2.3). The only major differences among the 3 sites was the amount of irrigation received. Carberry was regularly irrigated, which contributed to the overall greater water inputs into the system when compared to the non-irrigated sites. Measured values of precipitation in-field compared to a non-irrigated system at Carberry collected from precipitation gauges indicated that 98.0 mm of total water inputs can be attributed to irrigation, leaving 160.9 mm of precipitation in Carberry, which is

Table 2.3 Characterization of the meteorological variables over the growing season.

	Carberry			Miami			Glenlea		
	Extreme	Average	Normal[1]	Extreme	Average	Normal[2]	Extreme	Average	Normal[3]
Maximum Temperature (ºC)	35.1 (August 12)	25.4	23.4	37.5 (August 12)	25.1	22.8	37.6 (August 12)	26.0	23.3
Minimum Temperature (ºC)	-2.3 (May 19)	10.9	9.2	0.1 (May 11)	13.2	10.4	-4.6 (May 10)	11.6	10.3
Average Wind Speed (m/s)	2.2			2.9			3.0		
Average Daily Solar Radiation (MJ/m^2)	21.3			23.9			22.6		
Growing Season	May 15 - August 22[4] (100 days)			May 11 – August 17 (99 days)			May 10 – August 14 (97 days)		
Total Growing Season Precipitation (mm)	161.0		269.8	148.0		293.6	147.8		325.3
Total Growing Season Irrigation (mm)	98.0			0			0		
Total Growing Season Reference Evapotranspiration (mm)	457.2			497.1			495.0		

[1]Climate normals are the 1981-2010 Brandon CDA data provided by Environment and Climate Change Canada (ECCC) for May 1 to August 31(Government of Canada, 2019a)

[2]Climate normals are the 1981-2010 Carman data for temperature normals and 1981-2010 Miami Orchard data for precipitation normals provided by ECCC for May 1 to August 31 (Government of Canada, 2019a)

[3]Climate normals are the 1981-2010 Glenlea data provided by ECCC for May 1 to August 31 (Government of Canada, 2019a)

[4]Carberry was not harvested until mid October due to inconvenient weather, but the crop was fully senesced by August 22, so the end of the growing season was assumed for this date

similar to precipitation at Miami (148.0 mm) and Glenlea (147.8 mm). Carberry also had a reference ET (Eq. 1) value approximately 40 mm less than the other two sites even with the longest growing season (Table 2.3).

The phenological development of the canola at the three sites followed a similar pattern (Table 2.4). The general pattern showed a quicker finish from the canola grown at Glenlea as development deviated from Miami after the flowering stage. The order to which the fields were seeded was the same as the order to which the crops were harvested (Glenlea, Miami, and Carberry). Growing degree days (GDD) for each growth stage were similar at all three sites, the greatest difference was at ripening, with a difference of 105 GDD between Glenlea and Carberry. Flowering was when GDD were the most similar with all three sites being within 46 GDD (Table 2.4). However, all the sites exceeded the GDD outlined by the North Dakota Agricultural Weather Network (NDAWN) for each stage of canola development (NDAWN, 2018).

Table 2.4 Canola development throughout the growing season at all 3 sites.

	Carberry (CMCDC)		**Miami (STC)**		**Glenlea (TGAS)**		**NDAWN GDD**
	Date Stage Recorded	Cumulative GDD	Date Stage Recorded	Cumulative GDD	Date Stage Recorded	Cumulative GDD	
Seeding Date	May 15		May 11		May 10		
Emergence	June 5[a]	248	June 5[a]	308	June 3[a]	279	0-142
Inflorescence Emergence	June 28	583	June 19	509	June 20	514	405-460
Flowering	July 6	688	June 27	642	June 29[b]	662	519-647
Seed Development	July 23	935	July 18	963	July 12	863	777-908
Ripening	August 10	1164	August 2	1156	July 26	1059	909-1041
Harvest	August 22[c]	1315	August 17	1398	August 15	1339	>1041

[a]First recorded crop staging, leaf development underway by this point.
[b]Estimated value. Flowering was not staged until seed development.

[c]Field was not harvested until mid-October. August 22 was a cut off for estimated harvest maturity.

The daily eddy covariance measured ET compared to daily ET generated from the unaltered FAO-56 Penman-Monteith equation, showed periods where minimal discrepancies existed and periods where large discrepancies existed throughout the growing season (Figure 2.2).

At Carberry, the closest agreement between modelled and measured ET was during the middle of the growing season, when the crop was close to reaching or had reached peak vegetative maturity. There were discrepancies between the model and measured ET within the first 30 days of the growing season (Figure 2.2) as the model did not seem to track the pattern of measured ET. Sums of the first 30 days for both modelled and measured ET were within 11 mm (63 mm was estimated and 52 mm was measured) so there was not necessarily an over/underestimation of the model at that point, as this worked out to be a difference of 0.37 mm day^{-1}. Within the last 20 days of the growing season, there was the largest source of discrepancies. There was a clear underestimation by the model as measured ET was sometimes 4 mm day^{-1} greater than modelled ET (Figure 2.2).

At Miami, the strongest relationship between modelled and measured ET was during the 3rd quarter of the growing season, this was when the crop was at peak vegetative maturity and going through the flowering stage. At the start of the growing season (the 1st quarter), there were discrepancies between the model and measured ET as modelled ET did not track the pattern of measured ET well (Figure 2.2). Between the 40th and the 50th day, there were overestimations by the model at some points as large as 3 mm day^{-1}. During the last quarter of the growing season, the model overestimated ET again, but not to the same extent seen earlier in the growing season.

At Glenlea, the strongest relationship between modelled and measured ET was during the 3rd quarter of the growing season, this was when the crop was at peak vegetative maturity and going through the flowering stage. Like the other two sites, the model in the first quarter of the growing season did not follow the same pattern as the measured ET. The model overestimated ET in the first 25 days by a cumulative value of 13.4 mm (Figure 2.2). Over the 2nd quarter of the growing season, the model follows the pattern of measured ET, but overestimated values of ET. Over the last quarter of the growing season, the model underestimated ET.

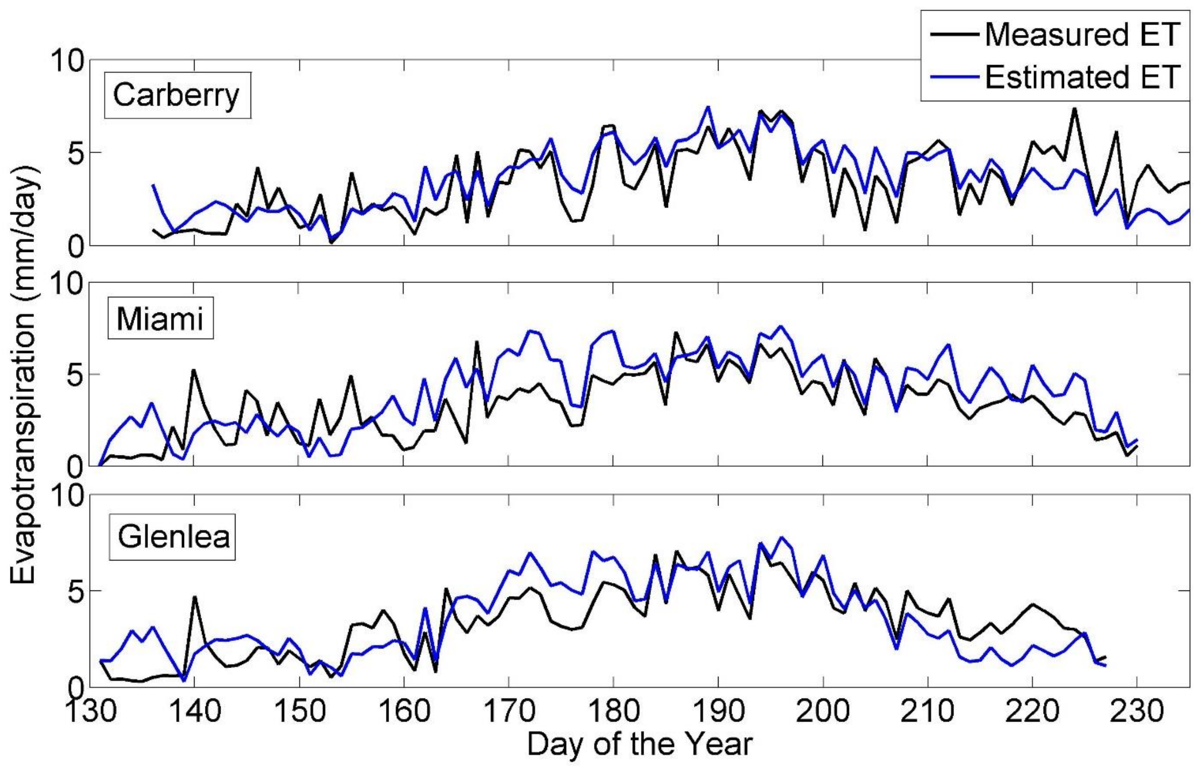

Figure 2.2 Comparison of eddy covariance measured and FAO-56 Penman-Monteith estimated actual ET at three sites of canola over the 2018 growing season.

2.6.2 Direct vs Indirect FAO-56 Penman-Monteith Model Inputs

Incorporating measurements of the difference between net radiation and ground heat flux, otherwise known as available energy, lessened differences between the FAO-56 Penman-

Monteith equation and the eddy covariance measured ET. Improvements to the R^2 value determined by comparing the estimated ET with the measured available energy to measured ET were 0.04 at Glenlea, 0.05 at Miami and 0.13 at Carberry. Root mean square error improved at Miami by 0.25 mm day^{-1}, while Glenlea and Carberry improved by 0.12 mm day^{-1}. Mean relative error improved by 12% at Miami, 10% at Carberry and 8% at Glenlea. The R^2, RMSE and MRE for each comparison of measured and estimated ET are outlined in Table 2.5 for each location. Major discrepancies were still present with the adjustment like the underestimation seen at the end of the growing season at Carberry (Figure 2.3). But most overestimations of the model were reduced such as the overestimations in the second quarter of the growing season at Miami and Glenlea (Figure 2.3).

Table 2.5 Combinations of FAO-56 Penman-Monteith improvement methods and R^2, RMSE (mm day^{-1}) and MRE (%) values and the linear equation when compared to measured actual evapotranspiration.

Measurement of Available Energy	**Dynamic Crop Coefficient**	**Water Stress Coefficient**	**Glenlea**			**Miami**			**Carberry**		
			R^2	RMSE	MRE	R^2	RMSE	MRE	R^2	RMSE	MRE
			0.60	1.27	61	0.45	1.53	64	0.46	1.25	52
•			0.64	1.15	53	0.50	1.28	52	0.59	1.13	42
	•		0.68	0.95	51	0.61	1.09	45	0.51	1.17	44
		•	0.57	1.36	62	0.49	1.54	64	0.53	1.27	52
•	•		**0.72**	**0.91**	**45**	0.63	**1.08**	**43**	0.64	**1.11**	**38**
•		•	0.61	1.25	55	0.53	1.30	53	0.63	1.17	44
	•	•	0.63	1.07	53	0.61	1.13	47	0.55	1.22	47
•	•	•	0.67	1.03	47	**0.64**	1.12	45	**0.65**	1.17	42

• signifies the use of this improvement method

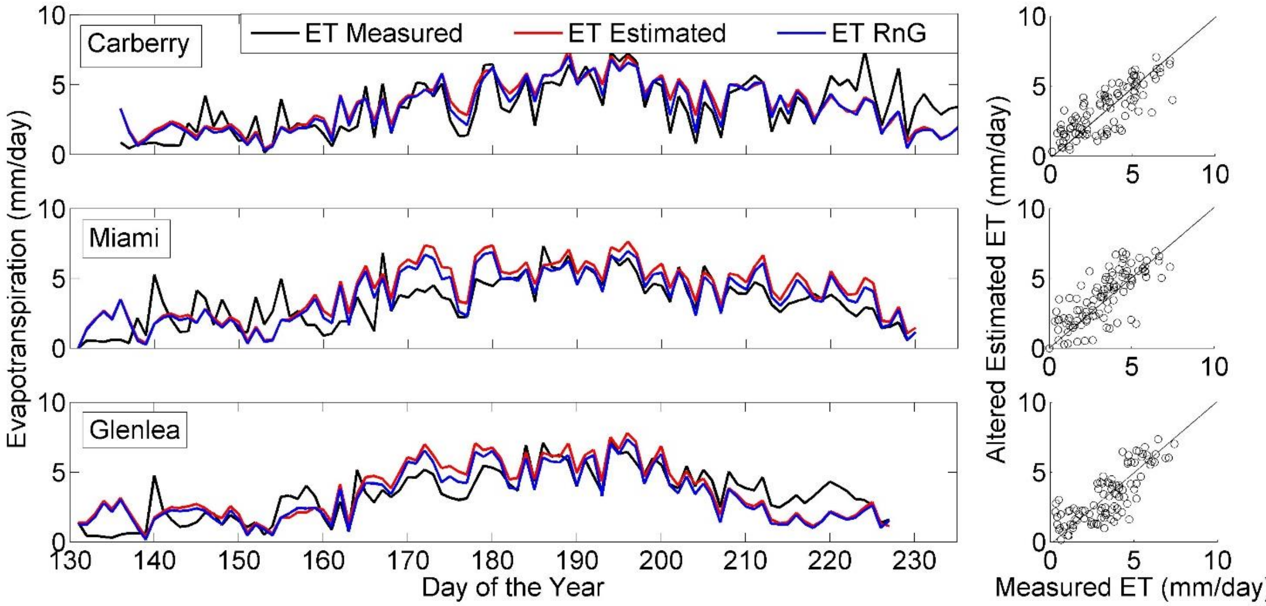

Figure 2.3 Comparison of actual ET determined by eddy covariance (ET Measured), unaltered FAO-56 Penman-Monteith equation (ET Estimated) and the FAO-56 Penman-Monteith equation with measured available energy (ET RnG). Regressions between adjusted estimated ET and measured ET for each site are additionally included with 1:1 lines shown.

2.6.3 Leaf Area Index Crop Coefficients (K_c)

Crop coefficients generated using LAI values are presented in Figure 2.4. These values generated by 3rd order polynomial equations (where x = day of the year) followed similar patterns with LAI peaking for Miami first, then Glenlea, then Carberry. Date ranges (or x-values) where these equations are applicable are 131-229 for Miami, 135-234 for Carberry and 130-226 for Glenlea. The polynomial equations are as follows:

Miami's LAI $K_c = -1.387 \bullet 10^{-6}\, x^3 - 2.6402 \bullet 10^{-5}\, x^2 + 1.6701 \bullet 10^{-1} x - 20.1328$

Carberry's LAI $K_c = -7.41 \bullet 10^{-7}\, x^3 - 2.08369 \bullet 10^{-4}\, x^2 + 1.7323 \bullet 10^{-1} x - 19.2333$

Glenlea's LAI $K_c = -1.0096 \cdot 10^{-5} x^3 + 5.064628 \cdot 10^{-3} x^2 - 8.2143 \cdot 10^{-1} x + 43.6055$

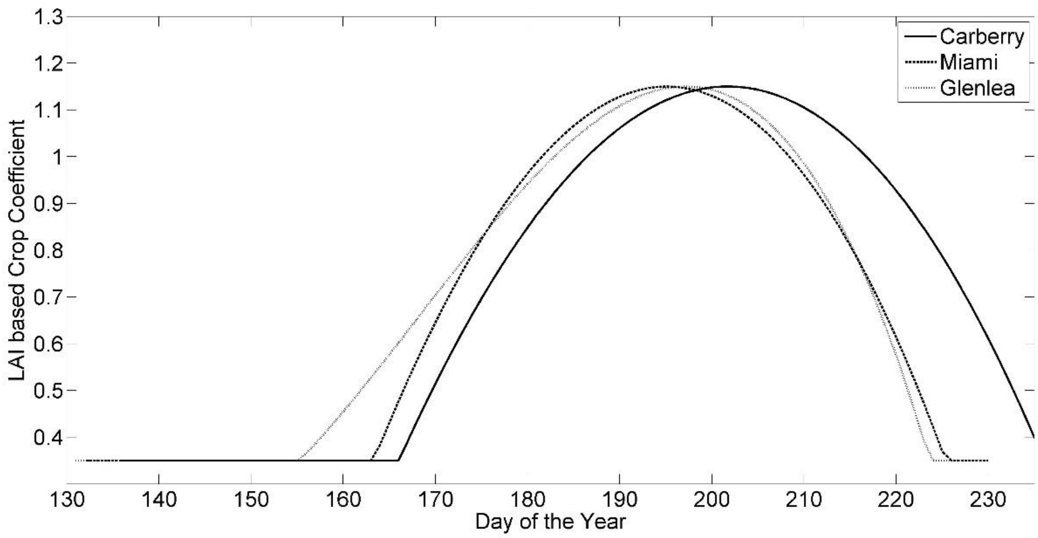

Figure 2.4 Crop coefficients (K_c) generated for each site of canola based on weekly leaf area index (LAI) measurements.

Measured LAI varied over the three sites. Differences in LAI at certain developmental stages are outlined in Table 2.6. All sites had their peak LAI at the seed development stage. Carberry had significantly greater LAI than Miami and Glenlea at this peak as Carberry had two units of LAI greater than the other two sites, but all three sites ended with similar LAI values at the ripening and harvest stages.

Table 2.6 Average leaf area index (LAI) and standard deviations for different phenological stages of canola at each site.

	Carberry (CMCDC)	Miami (STC)	Glenlea (TGAS)
Inflorescence Emergence	3.5 ± 0.97	1.6 ± 0.40	2.2 ± 0.24
Flowering	5.0 ± 0.95	2.4 ± 0.51	2.9 ± 0.27
Seed Development	5.8 ± 0.15	3.8 ± 0.50	3.8 ± 0.21
Ripening	3.0 ± 0.20	3.5 ± 0.38	3.0 ± 0.51
Harvest	2.4 ± 0.36	2.3 ± 0.14	2.7 ± 0.36

Incorporating a dynamic crop coefficient generated from weekly measurements of LAI into modelled ET values reduced discrepancies for all locations to varying degrees. At Miami, R^2 values increased by 0.16 when comparing estimated ET with a dynamic crop coefficient to measured ET. At Glenlea, R^2 increased by 0.08 and at Carberry, R^2 increased by 0.05. Root mean square error improved by 0.44 mm day^{-1} at Miami, 0.32 mm day^{-1} at Glenlea and 0.08 mm day^{-1} at Carberry. Mean relative error improved by 19% at Miami, 10% at Glenlea and 8% at Carberry. Large overestimations of ET were nearly completely removed in Miami and Glenlea during the 2nd quarter of the growing season (Figure 2.5). Underestimation by the model was still present near the end of the growing season for Carberry, but at Glenlea, the underestimation was reduced with the incorporation of a dynamic K_c. Overestimation by the model at the end of the growing season for Miami was also reduced.

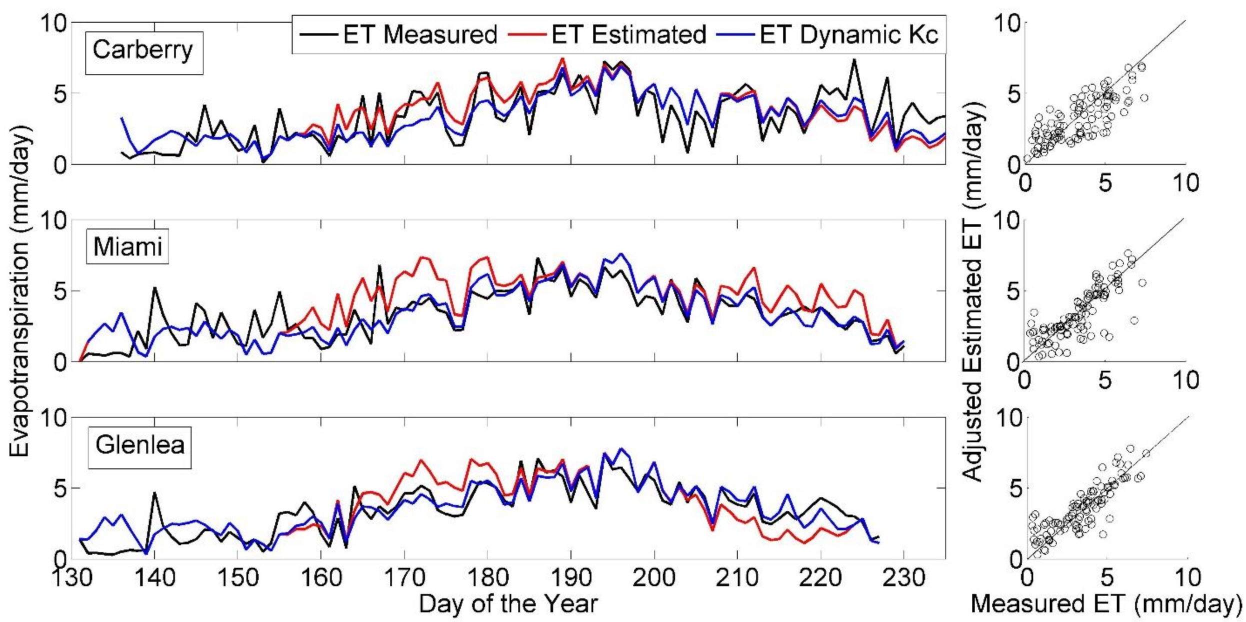

Figure 2.5 Comparison of actual ET determined by eddy covariance (ET Measured), unaltered FAO-56 Penman-Monteith equation (ET Estimated) and the FAO-56 Penman-Monteith equation with leaf area index (LAI) generated crop coefficients (ET Dynamic K_c). Regressions between adjusted estimated ET and measured ET for each site are additionally included with 1:1 lines shown.

2.6.4 Water Stress Coefficients

Water stress coefficients generated using the FAO method revealed that throughout the majority of the growing season at all three sites, the crops did not experience any moisture stresses. At Glenlea and Miami, only the first three days after emergence yielded results that suggested water stress. For Carberry, the first six days after emergence suggested water stress even though the system was irrigated. The majority of days that signified water stress suggested that the plant was so stressed that ET would be at the absolute minimum, which was set at 0.1 (Alberta Agriculture and Forestry, 2013). Values between 0.1 and 1 were seen only once out of the 3 sites, which was at Carberry on May 19th (0.40). Since there were minimal days that the crops were stressed due to lack of moisture, there were minimal changes in ET. Changes in R^2 seen by implementing a water stress coefficient were an increase of 0.04 at Miami, an increase of 0.07 at Carberry and a decrease of 0.03 at Glenlea. Root mean square error worsened by 0.01 mm day^{-1} at Miami, 0.02 mm day^{-1} at Carberry and 0.09 mm day^{-1} at Glenlea. Mean relative error was unchanged at Carberry and Miami, but was worsened at Glenlea by 1%. The stress coefficients that were less than unity were at a period of model overestimation for Carberry between day 155-162 and Miami between day 155-158, while at Glenlea from 154-156 they were in a period of model underestimation (Figure 2.6). At the end of the growing season at Carberry, the unaltered model underestimated ET already, and the incorporation of a stress coefficient further decreased ET, increasing the bias.

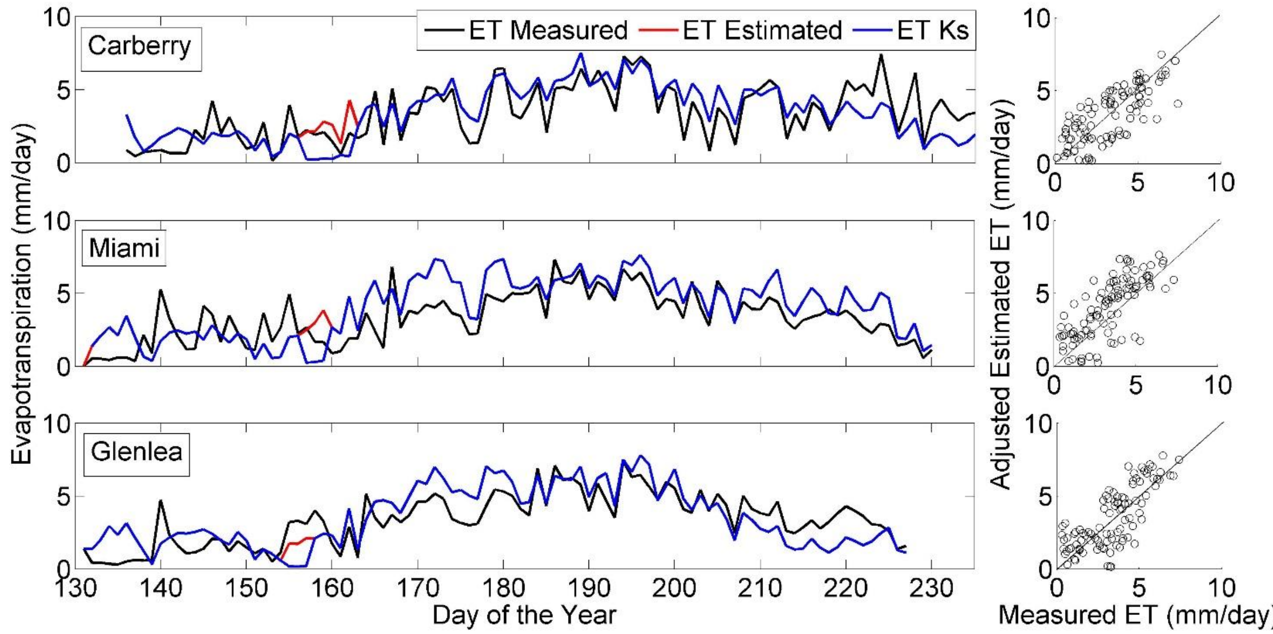

Figure 2.6 Comparison of actual ET determined by eddy covariance (ET Measured), unaltered FAO-56 Penman-Monteith equation (ET Estimated) and the FAO-56 Penman-Monteith equation with a water stress coefficient (ET K_s). Regressions between adjusted estimated ET and measured ET for each site are additionally included with 1:1 lines shown.

The water stress coefficient expressed stress when the coefficient was less than 1 and therefore was applied to estimated ET when the root zone depletion was greater than the readily available water. Figure 2.7 shows that apart from the initial days after emergence, readily available water was always greater than the root zone depletion. This makes it clear that for sites like Miami, the location was closer to experiencing water stress than sites like Carberry, as the gap between readily available water and root zone depletion was smaller for Miami (26 mm) than Carberry (260 mm) at the end of the growing season.

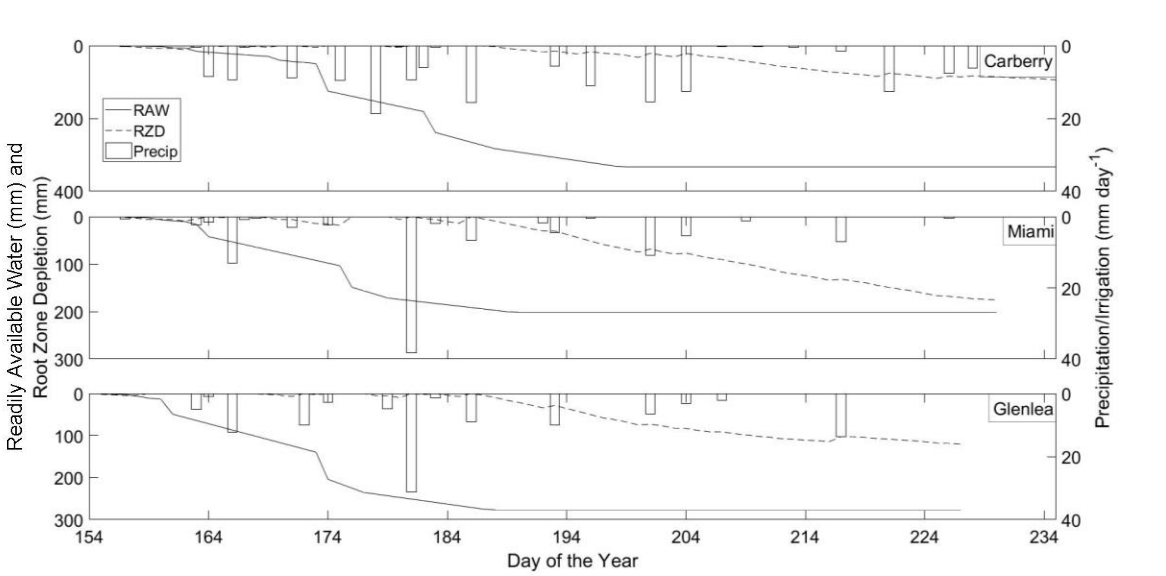

Figure 2.7 Balance of readily available water (RAW) and root zone depletion (RZD), as well as daily precipitation (Precip) at all 3 sites.

2.6.5 Full Comparison

When comparing the various improvement methods to the FAO-56 Penman-Monteith equation of directly measured available energy, a dynamic crop coefficient, and a water stress coefficient, there was an additive impact with the addition of 2 or more improvement methods at the same time. The largest improvement of the model using R^2 values was when all 3 improvement methods were implemented for Carberry and Miami, and when a water stress coefficient was excluded at Glenlea as outlined in Table 2.5. The improvements in R^2 between the unaltered FAO-56 Penman-Monteith equation to the equation with the optimum combination of adjustments were 0.12 for Glenlea, 0.19 for Miami, and 0.19 for Carberry. The greatest improvements in RMSE and MRE were seen when only measured available energy and the dynamic crop coefficient were included, and the water stress coefficient was excluded. The improvements in RMSE between the original FAO-56 Penman-Monteith equation to the equation with the optimum combination of adjustments was 0.45 mm day^{-1} at Miami, 0.36 mm day^{-1} at Glenlea, and 0.14 mm day^{-1} at Carberry. The greatest improvements for MRE were 21% at Miami, 16% at Glenlea and 14% at Carberry.

Cumulative estimated ET using various methods and combinations of improvements tracked the general pattern of measured ET throughout the growing season. Figures 2.8, 2.9 and 2.10 show that the majority of adjusted models had ET within the 10% thresholds above and below the measured ET. In all instances, the original FAO-56 Penman-Monteith equation gave greater ET than the upper threshold for more than half of the growing season.

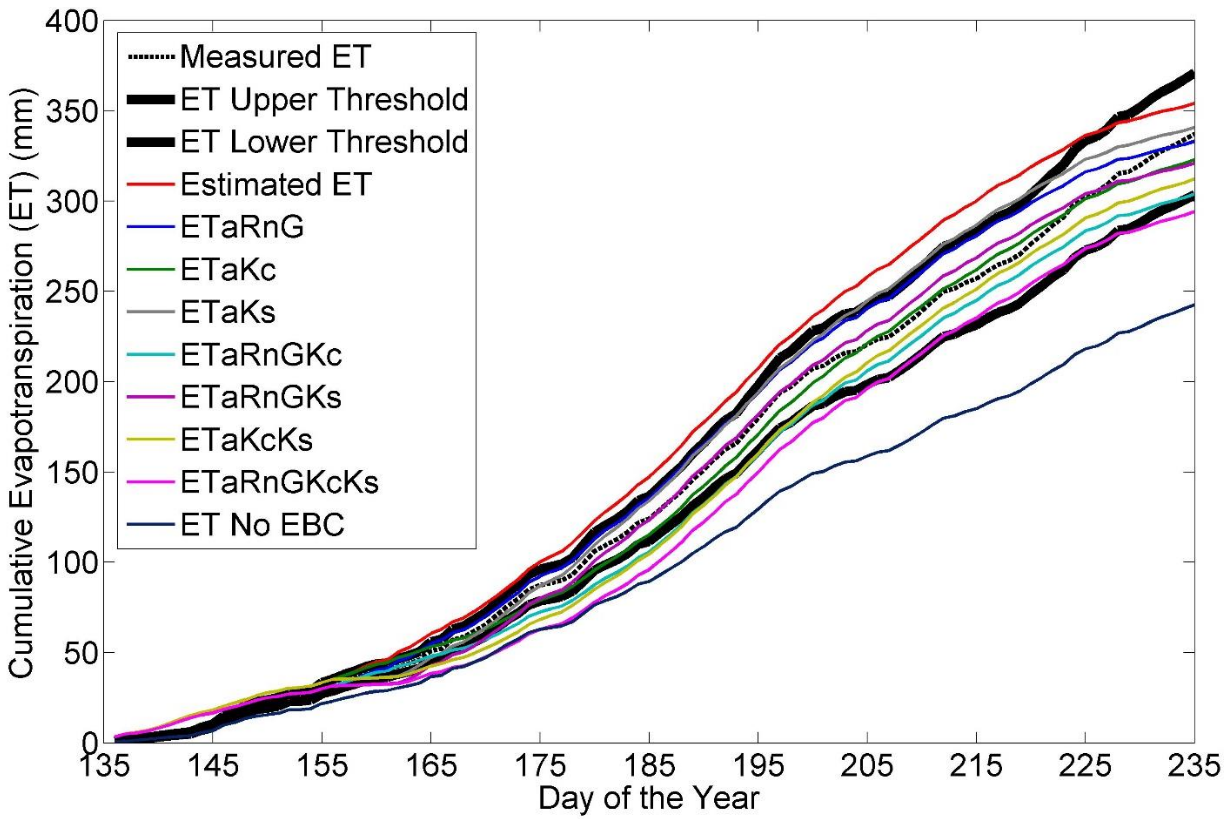

Figure 2.8 Comparison of cumulative measured and estimated ET adjusted with a combination of methods for the Carberry site. Methods include measured available energy (RnG), a LAI based crop coefficient (K_c) and a water stress coefficient (K_s). Upper and lower thresholds represent 10% error associated with eddy covariance ET measurements. Measured ET without energy balance closure is also provided (No EBC).

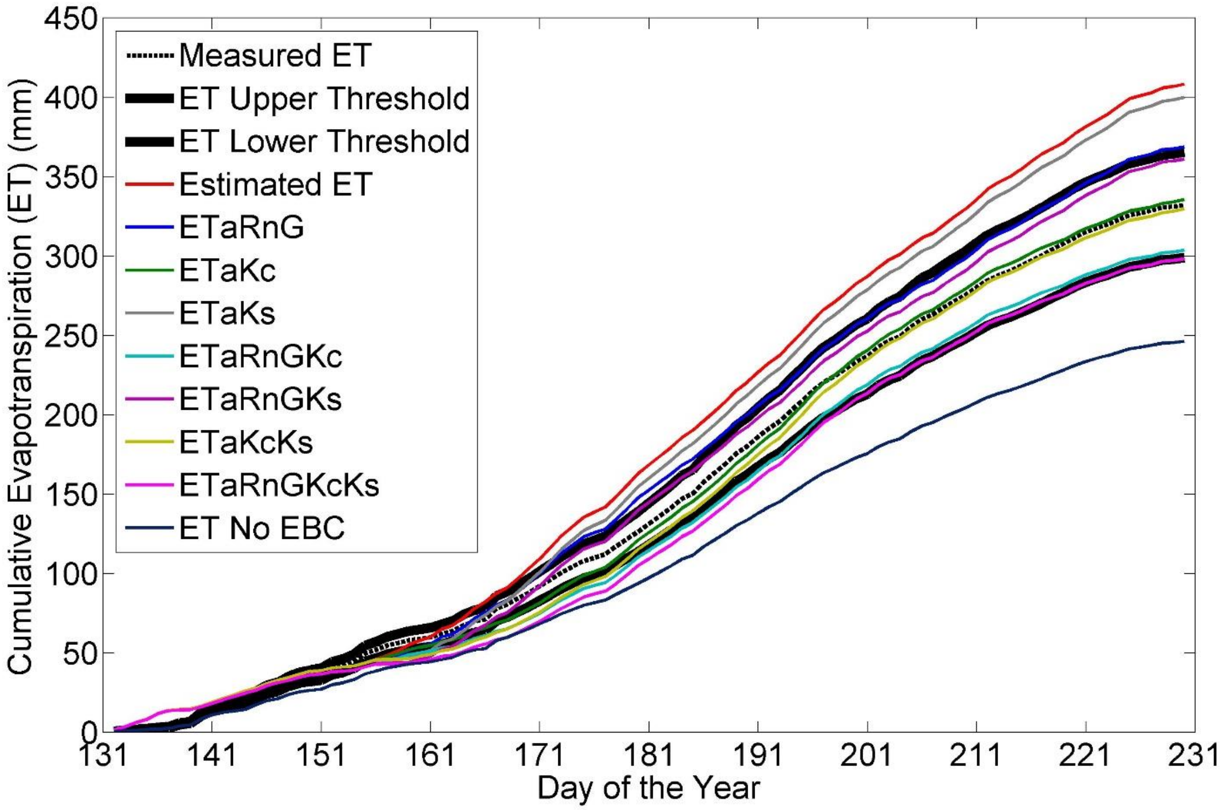

Figure 2.9 Comparison of cumulative measured and estimated ET adjusted with a combination of methods for the Miami site. Methods include measured available energy (RnG), a LAI based crop coefficient (K_c) and a water stress coefficient (K_s). Upper and lower thresholds represent 10% error associated with eddy covariance ET measurements. Measured ET without energy balance closure is also provided (No EBC).

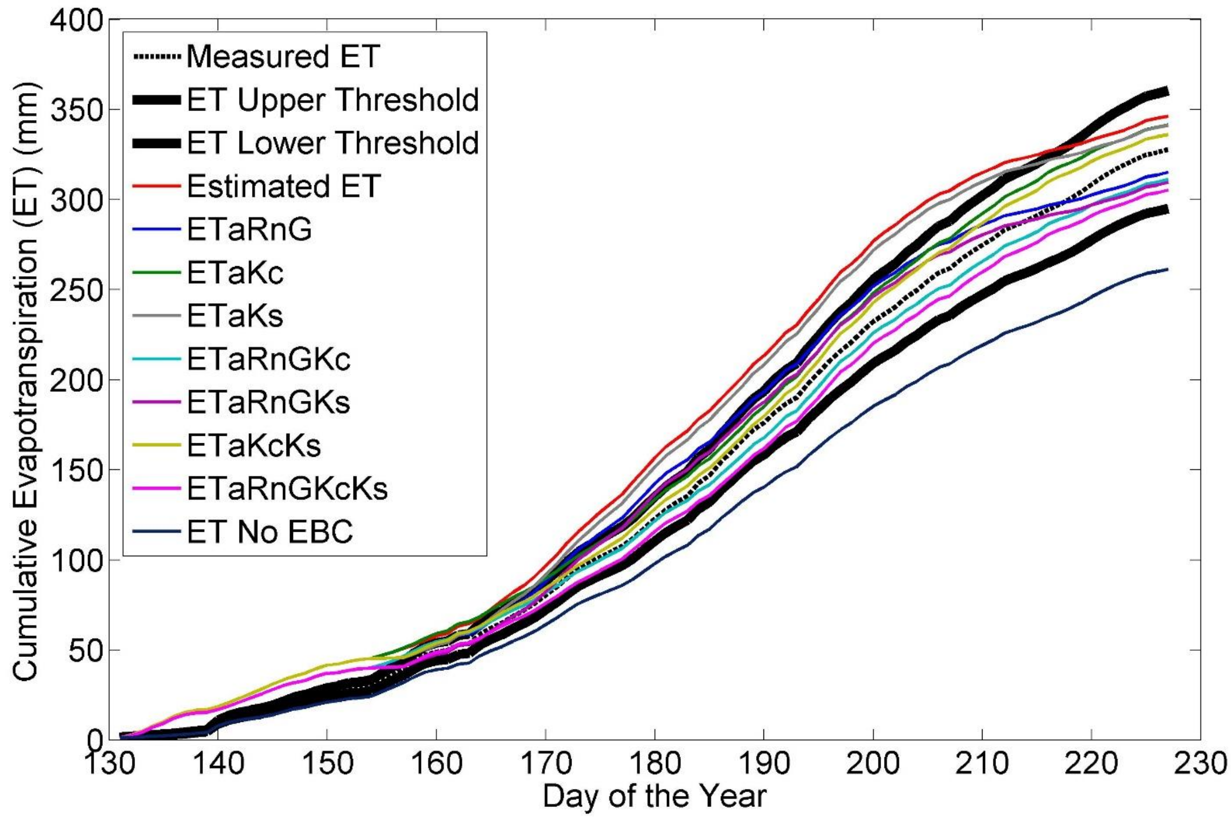

Figure 2.10 Comparison of cumulative measured and estimated ET adjusted with a combination of methods for the Glenlea site. Methods include measured available energy (RnG), a LAI based crop coefficient (K_c) and a water stress coefficient (K_s). Upper and lower thresholds represent 10% error associated with eddy covariance ET measurements. Measured ET without energy balance closure is also provided (No EBC).

Values of measured ET without energy balance closure on Figures 2.8, 2.9 and 2.10 show that in all instances, not using an energy balance closure procedure yielded cumulative ET values below the lower 10% threshold based on measured ET using a forced energy balance closure. Totals of ET without forced energy balance closure were 243 mm at Carberry, 246 mm at Miami, and 261 mm at Glenlea over the same growing seasons seen for measured ET totals with forced energy balance closure. In order to force energy balance closure, multipliers of 1.39 at Carberry, 1.35 at Miami, and 1.26 at Glenlea had to be applied to measured latent and sensible heat fluxes. This showed that 28% of ET at Carberry, 26% of ET at Miami, and 20% of ET at

Glenlea that was measured over the growing season was attributed to forcing energy balance closure with the multiplier assigned for each site.

Improvements to the model were broken down into 30-day periods in the growing season distinguished as initial, middle and end to show where the greatest error occurs, as well as where large improvements occur. Tables 2.7, 2.8 and 2.9 outline that the most improved model was mostly the combined measured available energy and dynamic K_c method regardless of the time of the growing season. Any other most improved method for a specific 30-day period was either the measured available energy single improvement or the dynamic K_c single improvement. Root mean square error was similar for all 3 periods of development. At Miami and Glenlea, the worst RMSE for the original model was the middle period, as this was the period with the over estimation of ET in the second quarter. Incorporating improvement methods helped improve the RMSE to a greater extent during this middle period at the two sites when compared to improvements seen during the initial 30-day period. Mean relative error was consistently greater for the initial 30-day period for all sites when compared to the middle or end 30-day periods.

Table 2.7 Root Mean Square Error (RMSE) (mm day^{-1}) and Mean Relative Error (MRE) (%) for each improvement method compared to measured ET in canola at Carberry, MB over the 2018 growing season.

	Growing Season		**Initial (May 15 – June 13)**		**Middle (June 14 – July 13)**		**End (July 14 – August 12)**	
	RMSE	MRE	RMSE	MRE	RMSE	MRE	RMSE	MRE
Unaltered	1.25	52	1.15	85	1.05	33	1.29	39
RnG	1.13	42	1.11	75	**0.80**	22	1.11	26
Kc	1.17	44	1.10	75	1.13	23	1.17	37
Ks	1.27	52	1.25	88	1.05	33	1.29	39
RnGKc	**1.11**	**38**	**1.09**	**68**	1.11	**20**	**0.97**	**25**
RnGKs	1.17	44	1.23	81	0.80	22	1.11	26
KcKs	1.22	47	1.29	86	1.13	23	1.17	37
RnGKcKs	1.17	42	1.29	81	1.11	20	0.97	25

Table 2.8 Root Mean Square Error (RMSE) (mm day^{-1}) and Mean Relative Error (MRE) (%) for each improvement method compared to measured ET in canola at Miami, MB over the 2018 growing season.

	Growing Season		**Initial (May 11 – June 9)**		**Middle (June 10 – July 9)**		**End (July 10 – August 8)**	
	RMSE	MRE	RMSE	MRE	RMSE	MRE	RMSE	MRE
Unaltered	1.53	64	1.63	122	1.85	49	1.07	23
RnG	1.28	52	1.59	115	1.47	35	0.72	15
Kc	1.09	45	**1.54**	111	**1.01**	19	0.72	13
Ks	1.54	64	1.66	123	1.85	49	1.07	23
RnGKc	**1.08**	**43**	1.54	**106**	1.03	**18**	**0.61**	**12**
RnGKs	1.30	53	1.64	117	1.47	35	0.72	15
KcKs	1.13	47	1.63	117	1.01	19	0.72	13
RnGKcKs	1.12	45	1.64	112	1.03	18	0.61	12

Table 2.9 Root Mean Square Error (RMSE) (mm day^{-1}) and Mean Relative Error (MRE) (%) for each improvement method compared to measured ET in canola at Glenlea, MB over the 2018 growing season.

	Growing Season		**Initial (May 10 – June 9)**		**Middle (June 10 – July 9)**		**End (July 10 – August 8)**	
	RMSE	MRE	RMSE	MRE	RMSE	MRE	RMSE	MRE
Unaltered	1.27	61	1.31	130	1.33	33	1.18	26
RnG	1.15	53	1.19	115	0.98	21	1.23	28
Kc	0.95	51	1.28	129	**0.76**	18	0.74	13
Ks	1.36	62	1.56	135	1.33	33	1.18	26
RnGKc	**0.91**	**45**	**1.16**	**115**	0.83	**15**	**0.64**	**12**
RnGKs	1.25	55	1.48	121	0.98	21	1.23	28
KcKs	1.07	53	1.54	135	0.76	18	0.74	13
RnGKcKs	1.03	47	1.46	121	0.83	15	0.64	12

2.6.6 Comparing Reference ET determined over a Grass Surface and In-Crop

Reference ET determined using the FAO-56 Penman-Monteith for a short grass reference crop on a daily basis was calculated using maximum and minimum temperature, maximum and minimum relative humidity, wind speed, and incoming solar radiation determined with meteorological equipment within the canola and meteorological equipment run by the Manitoba

Agriculture Weather Program over a grassed surface 660 m west of the in-field measurements. Differences between reference ET measured in-crop and over a grass surface were compared (Figure 2.11). The R^2 value of this comparison was 0.95. Consecutive days with greater than 1 mm day^{-1} difference in reference ET between the two surface types occurred on day 223-224 (Figure 2.11). The largest difference was on day 228 when reference ET over the grass was greater than reference ET in the canola by 1.21 mm. Other days throughout the growing season with differences greater than 1 mm day^{-1} between the two reference surfaces were day 195 and 203. Total growing season cumulative reference ET was 457 mm in-crop and 466 mm over the grassed surface which is only a 2% difference in reference ET.

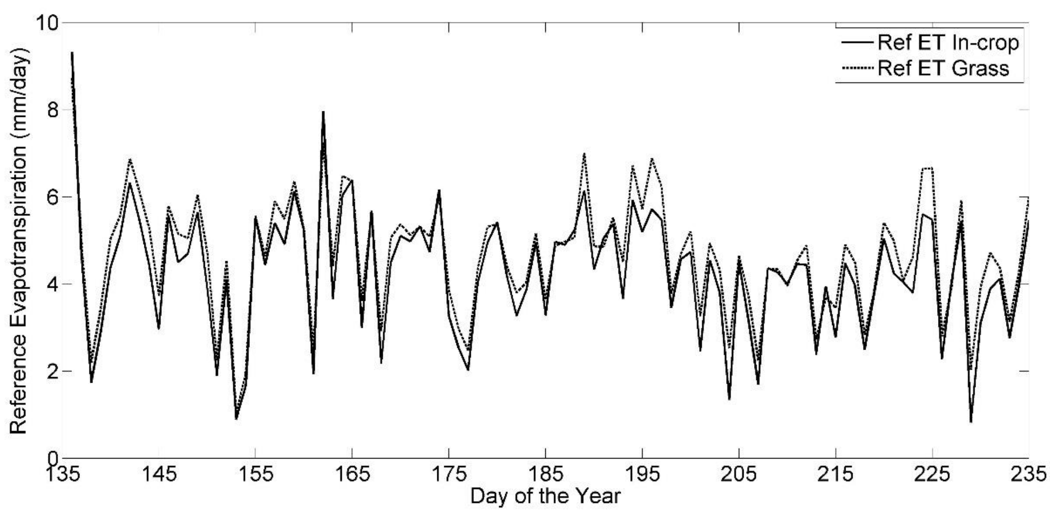

Figure 2.11 Reference ET estimated in the canola (Ref ET In-crop) and over a reference grass surface (Ref ET Grass) using the FAO-56 Penman-Monteith equation at the Carberry site.

2.7 Discussion

2.7.1 Difference between Eddy Covariance and FAO-56 Penman-Monteith Method

Differences in ET generated by a model and through actual ET measurements can ultimately be due to the challenge of using basic meteorological variables to determine a complex process like ET (Martel et al., 2018). The various estimation techniques can yield different results at the same location, and techniques can vary in accuracy in different climatic locations (Allen et al., 1998). Temperature, relative humidity, wind speed and incoming solar radiation all have an effect on ET, but translating their effect through an equation to represent every agroecosystem can be challenging. For the FAO-56 Penman-Monteith equation, there were problems with representing actual ET with the model; one of these problems was at the start of the growing season.

For the majority of the growing season, the model could follow the pattern of measured ET even if there was an over/underestimation by the model. But at the start of the growing season, there was trouble with the model tracking actual ET (Figure 2.2). This inability to track ET at the start of the growing season was likely due to precipitation events and the lack of transpiration occurring. As precipitation was not a variable considered by with the model (Allen et al., 1998), and precipitation contributes to rates of ET, it would make sense that measured ET would change with precipitation events with no measurable response in the model, similar to what was observed on day 140 at Miami and Glenlea. Precipitation brings cloud coverage, which would limit incoming solar radiation and rain helps reduce air temperature and increase relative humidity. These effects of precipitation are accounted for by the model as they indirectly effect weather parameters defined in the model (Allen et al., 1998). But increased levels of surface moisture that will be exposed to incoming solar radiation after the clouds have passed is not considered in the equation. A greater surface moisture content will lead to greater rates of evaporation when exposed to solar radiation, which cannot be predicted in the FAO-56 Penman-Monteith equation. This inability to track measured ET at the start of the growing season would suggest a problem in the determination of ET when the process is dominated by evaporation

(Martel et al., 2018). When considering the original Penman equation focused on predicting evaporation, it looked at pan evaporation, which is quite simplified when compared to evaporation from a soil surface (Penman, 1948). Factors including soil texture, organic matter and soil colour all contribute to the rates of ET, something that is not considered when determining ET from an open water body when using the Penman equation. These differences between evaporation from an open water body and a soil system could be a reason why ET has lower agreement with measured ET when evaporation is the dominant process during the growing season. At the start of the growing season, there should not be much transpiration, as emergence has not occurred or emerged plants are still in juvenile stages of development. Later on in the growing season when plants were further along in development and transpiration contributes more to total water vapour losses, there was a greater ability to follow measured patterns of ET. In theory, transpiration rates should not be affected by increases and decreases in available moisture, as long as there's sufficient amounts of moisture for proper development, which is when the soil system's moisture content is between field capacity and the permanent wilting point (Verstraeten et al., 2008). Transpiration is more directly controlled by stomatal conductance and the pattern of incoming solar radiation. Evaporation is directly influenced by the amount of water available to evaporate from within the topsoil and water intercepted on plant surfaces, and therefore is directly affected by precipitation events (Verstraeten et al., 2008).

At Carberry, modelled ET follows measured ET throughout the middle of the growing season, but near the end of the growing season, there was an underestimation of ET (Figure 2.2). This could be due to late-season irrigation events. At this point of the growing season, transpiration was limited. The canola was senescing or completely senesced so most water vapour losses were from evaporation. The environment at this point of the growing season was ideal for evaporation (low relative humidity, above average temperatures, and sunny), so inputs of moisture would be easily evaporated. When irrigation occurred, there was an increased rate of ET as a response that's not directly captured by the model, as the model does not use inputs of moisture to determine rates of ET. Values of vapour pressure deficit ($e_s - e_a$) capture some of the effects of irrigation as relative humidity increases with the presence of irrigation, but as mentioned before, the model has difficulty representing ET when evaporation is the dominant process, regardless of moisture inputs like rainfall or irrigation.

At Miami, modelled ET was overestimated during the second quarter of the growing season (Figure 2.2). This could be due to 2 possibilities, the first being lower than normal plant densities, and secondly could be due to drought stress. Miami had almost half the final plant density compared to Carberry (Table 2.1). A major difference between the two sites that could have led to this discrepancy in plant density was the presence of flea beetles (*Phyllotreta cruciferae*). Flea beetles feed on species in the Mustard family (*Brassicaceae*) across the Canadian prairies, and usually impose the biggest impact on canola at the cotyledon and first true leaf stage, with almost no effect on yield after the fourth leaf stage (Lamb, 1984). With feeding on the juvenile plants, there is a decrease in photosynthetically active plant biomass, and therefore lower transpiration rates compared to a crop under no pest stresses. Miami was affected by flea beetles early in the growing season (first noticed during emergence), which limited the plant stand and biomass development of the canola. Carberry also had a presence of flea beetles, but had the benefit of opportune spraying and irrigation to limit the pest's effects on the crop. Although presence of flea beetles were seen within the first quarter of the growing season, effects on ET were not seen until further in the growing season. During this 2nd quarter of the growing season, biomass development differed to a greater extent in comparison to a normal plant density at that growth stage than in the 1st quarter of the growing season. This greater photosynthetically active plant biomass difference contributes to a greater difference in transpiration rates, as quantity of plant biomass that can transpire and the rate of transpiration from a system are directly correlated. Plant density is not a factor used to estimate ET through the FAO-56 Penman-Monteith equation (Allen et al., 1998), so lower than standard plant densities caused by the impact of flea beetles could lead to the model overestimating actual ET.

Drought stress could also be a contributing factor for overestimation by the model. Within the second quarter of the growing season, there was only 11.4 mm of precipitation until June 30th when there was 38.3 mm of precipitation. During the first quarter of the growing season, there was 45.1 mm of precipitation. From May 1, 2017 to May 10, 2018 (day before seeding), there was a total of 366 mm of precipitation at the Deerwood Environment and Climate Change Canada weather station (Government of Canada, 2019b), which was 67% of the normal precipitation of the nearby town of Carman, MB (MAWP, 2018). This suggests lower than normal inputs of moisture, so lower than normal precipitation in the following year could create drought conditions and suggest the overestimation by the model for this period. Drought stress was not directly seen with a water stress coefficient during these periods of the growing season at Miami, but low moisture values present in the soil could still contribute to low ET values until the June 30th precipitation event.

The biggest discrepancy between modelled ET and measured ET for Glenlea was at the end of the growing season, approximately around August 4th (Figure 2.2). The sources of discrepancies were likely either due to a large precipitation event near the end of the growing season, or a desiccant application. On August 4th, there was a precipitation event of 13.7 mm. At this point of the season, similar to the start of the growing season, transpiration was minimal.

The majority of water vapour released to the atmosphere from a field was in the form of evaporation. This precipitation event could have fuelled evaporation and actual ET greater than the model predicted, as the model does not directly consider precipitation. The other method that could lead to underestimations of ET could be a desiccant application on August 9th. Applying a paraquat desiccant can help complete senescence more quickly by allowing the moisture content of mature, senescing canola to decrease by 3% per day as compared to 1.75% per day without any desiccant (Esfahani, 2012). This releases greater than normal rates of water vapour from the crop at that growth stage, which would not be predicted by the model.

In order for the greatest improvements to the models representation of actual ET, areas with the greatest discrepancies need to be addressed by the improvement methods. Therefore, greater care must be placed on improvement methods for periods of vegetative growth and senescence, as this was where the greatest relative discrepancies occurred.

2.7.2 Directly Measured Available Energy

Incorporating directly measured available energy (net radiation – ground heat flux) improved the model at all 3 sites. Within the FAO-56 Penman-Monteith model itself, net radiation and ground heat flux are derived from incoming solar radiation. Incoming solar radiation is a main contributor to net radiation and along with an assumed albedo, incoming solar radiation can be used to predict net radiation with confidence, assuming the albedo of 0.23 is representative of the actual crop surface (Allen et al., 1998). Ground heat flux, although smaller than net radiation typically, is harder to predict. In some work, ground heat flux is proportioned at 0.3x the net radiation for sparse canopies (Brutseart, 1982), but this value can vary depending on the agroecosystem. Within the Penman-Monteith equation, ground heat flux is assumed to be zero as it is far smaller than net radiation (ground heat flux rarely reaching greater than 2 MJ m^{-2}

day at all sites). But soil heat flux plates provide a direct measurement of ground heat flux that can be used to help represent energy dynamics within the agroecosystem better. Incorporating direct measurements of available energy at all three sites decreased measured daily ET over the growing season as estimated ground heat flux was assumed to be zero and measured values were typically positive. With a positive measured value of G, it makes sense that ET would decrease. As Rn-G is available energy, when ground heat flux increases, available energy decreases (Santanello Jr. & Friedl, 2003). This improved measured ET as the model overestimated ET during the middle of growing season for all sites. This overestimation was minimized by the incorporation of measured values during this time, and had a greater impact than when the model worsened with the addition of available energy near the end of the growing season where the model underestimated ET. As an assumed surface albedo is less representative of a field of canola near the beginning and end of the growing season when there is less plant biomass and more exposed soil surface, and as ground heat flux is the greatest when there is more exposed soil, the adjustment to the model should provide the greatest impact during these parts of the growing season. Differences between measured and estimated ET at these times are not observably large as rates of daily ET are lower at these points of the growing season when compared to the middle of the growing season. So even though the model was changed with a greater magnitude by incorporating measured available energy at the start and end of the growing season, it does not generate as much of a difference in mm day^{-1} of moisture seen in the middle of the growing season.

2.7.3 Dynamic Crop Coefficients

Using LAI to help represent crop development improved the model for all 3 sites, but mostly for Miami. The reason for such improvements was due to the impact on crop coefficients that lowered the estimated ET in periods of overestimation like during the second quarter of the growing season and near the end of the growing season (Figure 2.5). The model only bases changes in ET from the four weather parameters and the FAO-56 crop coefficient which changes with crop staging, it does not directly consider plant density and photosynthetically active biomass in its measurements (Gardiol et al., 2003). Gardiol et al., (2003) compared two densities (22000 and 91000 plants•ha^{-1}) of maize (*Zea mays*) to test estimation techniques including the FAO-56 Penman-Monteith equation and found large differences in ET and LAI. The lower plant density accumulated 386 mm of ET compared to the higher crop density's accumulation of 551 mm over the same time period. The Penman-Monteith equation estimated a value of 539 mm, which was similar to the higher plant density's value of ET but a 153 mm overestimation of ET for the maize with a lower plant density. Peak leaf area index values for each field was 1.5 for the lower plant density and 5.5 for the higher plant density. This information suggests that the FAO-56 Penman-Monteith equation could reflect ET for fields of different plant densities if leaf area index values are incorporated, as leaf area index in this situation clearly reflects differences in the two agroecosystems.

As previously mentioned, during the 2nd quarter of the growing season, Miami's canola was still dealing with the effects of the flea beetles presence during the first 2 weeks after emergence. This field was going through the same pattern of development as the other fields, but plant density was observably lower. So, we saw a greater estimated ET for this time period as the model assumed the canola was at a greater plant density than what was actually present. Using the LAI value to develop crop coefficients took into consideration the plant densities, so it could represent ET better throughout these periods of overestimation. A similar case in plant density was assumed at Glenlea over the 2nd quarter of the growing season. At both Miami and Glenlea, the use of LAI based crop coefficients improved agreement between measured and modelled ET in the 2nd quarter of the growing season. Since there was lower plant density that was overlooked with the FAO-56 crop coefficients and captured with the LAI based crop coefficients, both Miami and Glenlea had large improvements with this model adjustment (increased r^2 by 0.16 (Miami) and 0.09 (Glenlea)).

It's important to note that this dynamic method was not purely based on measured values. Leaf area index measurements could not be taken at the initial stages of the canola's growth cycle. The LAI-2200 (LI-COR Inc., Lincoln, NE) needs sufficient space between the optical lens and the leaf in order to take accurate LAI measurements (LI-COR, 2013). The recommended distance is 4x the width of the leaf. This could not be achieved until early June. Throughout May, there was photosynthetically active vegetation which could contribute to ET, but it was not developed enough to measure leaf area index and therefore determine a dynamic crop coefficient for. By using just measurements of LAI to determine a dynamic crop coefficient, the initial K_c stage was representing canola development too far into the growing season, causing large underestimations by the model. For Carberry around day 165, there was a difference between measured ET and the modelled ET with a dynamic coefficient. At this point the FAO K_c value was in its developing stages, as it was about 0.66 but the dynamic K_c was still at 0.35 (Kc initial). In fact, the dynamic K_c value did not increase until day 173. By the time the FAO Kc value hits 1.0, the dynamic K_c value was at 0.50. From between 165 and 173, actual K_c ranged from 0.33 to 1.02 with only one value (0.33) being under 0.5. This is why an estimated value of LAI generated from estimated height was incorporated into the polynomial equation so the equation could better represent biomass development and ET for this growing season.

2.7.4 Water Stress

Determining a water stress coefficient using soil moisture content and the FAO-56 stress coefficient method showed that there was little to no water stress at any of the sites. It was expected at Carberry to have the least amount of water stress as it was irrigated adequately, receiving inputs at opportune times (during flea beetle infestations and flowering) to ensure the highest productivity. But the FAO-56 stress coefficient actually determined during the initial stages of the growing season that the highest water stress occurred at Carberry. The suspected difference could be due to the difference in soil type. Carberry is mainly Ramada and Wellwood Soil Series which have a higher percent sand content and have a lower field capacity (Knutson, 2017). Field capacity at Carberry ranged from a volumetric moisture content of 38% to 30% within the first 80 cm and from 80 cm went down to 9% in some places (Government of Canada, 2013). Field capacity at Glenlea ranges from a volumetric moisture content of 44% to 47% in the first 100 cm of depth and the field capacity of Miami's soil ranged from a volumetric moisture content of 34-40% in the first 100 cm. Available water holding capacity (AWHC) at the three locations was the lowest at Carberry, ranging from a volumetric moisture content of 14 to 17% in the first 80 cm and then being as low as 2% from 80 cm and lower. Glenlea's AWHC ranged from a volumetric moisture content of 21 to 22% while Miami had an AWHC of 17 to 19%. This suggests that there is less ability for the soils at the Carberry site to hold moisture and therefore are at greater risk of seeing drought stresses than soils at Glenlea and Miami with the same moisture inputs. Therefore, even though there were greater inputs of moisture at Carberry, the presence of moisture stress can still occur and not be present at Glenlea or Miami.

An interesting pattern in these data was when there was a presence of moisture stress signified by a stress coefficient, it did not necessarily correlate with the suspected moisture stresses from the pattern of actual ET and modeled ET that we had seen previously. Water stress was suspected at Miami during the lull in measured ET during the 2nd quarter of the growing season. But during this period, there was no sign of stresses using the FAO-determined stress coefficients. Stresses were only seen at the initial stages of development after emergence using the FAO-56 stress coefficient. Since the stress coefficient uses rooting depth as an indicator of how much available water there is for plant uptake, and initial estimated rooting depths are so shallow, it leads to a readily available water (RAW) value that's quite low, typically lower than what would be lost from the system through ET (Allen et al., 1998). As precipitation and ET are main drivers for root zone moisture and there was minimal precipitation with 2-3 mm day^{-1} of ET, root zone depletion was typically higher than the readily available water. For the rest of the growing season, the readily available water was greater than the root zone depletion, as the rooting depth increased and could obtain moisture at deeper depths.

It is thought that the FAO-56 Penman-Monteith equation has problems representing moisture stress. A comparison between the Prairie Agrometeorological Model (PAM2nd) and the FAO-56 Penman-Monteith equation for ET and soil moisture over spring wheat showed that the PAM2nd model was better at representing dry-season soil moisture than the FAO-56 Penman-Monteith equation, but still attributed to an overestimation of soil moisture during the second half of the growing season (Gervais, 2009). This suggests that the FAO-56 Penman-Monteith equation could be overestimating the amount of soil moisture there is in the soil. There could be water stress present near the end of the growing season in Miami, and as the water stress coefficient overestimates ET, it doesn't signify that there is stress present.

2.7.5 Combined Impact of Improvement Methods

As incorporating the improvement methods of directly measured available energy, dynamic crop coefficients, and water stress coefficients individually all improved the R^2

relationship between measured actual ET (except the water stress coefficient at Glenlea), the incorporation of all 3 improvement methods improved the R^2 relationship the greatest at 2 of the 3 sites. Incorporating the water stress coefficient decreased agreement between measured and modelled ET based on RMSE and MRE. With the degree of improvement outlined in Table 2.5, the consistency between each method and how much of an impact it had was different for each site. No method yielded the greatest R^2, RMSE and MRE improvement for all 3 sites, so it's difficult to identify a single improvement method that would be most effective everywhere. Implementing an improvement method might not be worth while depending on the person/purpose for ET estimation as implementation and maintenance can be costly and time-consuming. The cost of implementing these improvements besides the cost of the equipment and the time spent setting-up and maintaining equipment would be the potential for no improvements of the model arising from these adjustments. The potential benefit of the adjustments would be if improvements were seen and it allowed producers to make better management strategies using values of ET which would end up making their crops more productive. If the combined improvement methods are incorporated at one site/weather station, and this information can be fully accessible to anyone, it will be worth it to producers around that weather station to use this information to make management decisions on their farm.

Determining which improvement methods to adopt should be based on the specific needs of the producer. The dynamic K_c value generated by LAI could be used when the stand of the canola is not necessarily standard (ex. Large row spacing, early season plant biomass loss) as this provided the greatest improvements to the model when plant density was low at Glenlea and Miami. If the producer is in a drought prone area, incorporating the water stress coefficient would be more useful than a producer that farms where drought is less common. Incorporating directly measured available energy improved agreement for all sites and for guaranteed improvements, this method would be the best to adopt.

2.7.6 Grassed vs In-crop Reference ET

Comparing reference ET generated for 2 weather stations within a kilometre from each other using the FAO-56 Penman-Monteith equation should yield nearly identical values of ET, assuming equipment used at both sites yields accurate values. By adding the variable of grassed versus cropped surfaces, there can be changes to weather variables used by the model between these two stations. For example, wind speed changes with the presence of a developed crop as it changes the surface roughness and therefore the aerodynamic characteristics that affects water vapour transport over the surface. This could contribute to the differences that were seen between reference ET measured over a grassed surface and in-crop. That's why it was important to compare the two, so if there was a question of proper representation using the FAO-56 Penman-Monteith in-crop even though the model is designed for a short grass surface, this comparison could help show the relevance of in-crop estimations using this method. Even though the differences were minimal, the differences could be the result of irrigation events, as the largest dissimilarities between the reference ET determined over a grassed surface and in-crop correlated with the day of or the day after irrigation took place on the crop (for example, day 223-224), and where there was no irrigation over the grassed surface (Figure 2.11). The irrigation event not only incorporated more water, but it drove down the daily maximum temperature by 2 to 3ºC through evaporative cooling (Liu & Kang, 2006). As temperature is a powerful driver in the FAO-56 Penman-Monteith equation, a decrease in 2 to 3°C can result in a drop in 1-2 mm of daily ET in the model.

2.7.7 Uncertainty

A u_* threshold of 0.1 m s^{-1} was applied to the measured ET at all the sites consistently throughout the growing season, even with changes in surface roughness. Using a standard u_* filter of 0.1 m s^{-1} was determined adequate as there were already various other methods of flagging and removing low quality data. A u_* threshold of 0.1 m s^{-1} has been used for various other similar agricultural systems (Anthoni et al., 2004, Baker and Griffis, 2005, Wilson et al., 2002), so this threshold can be used on the eddy covariance flux sites with confidence. Data were removed with the u_* filter as R^2 values between data with and without the filter were 0.9981 for Glenlea, 0.9978 for Miami, and 0.9986 for Carberry. Friction velocity values that went below the threshold of 0.1 m s^{-1} were 686/4656 data points at Glenlea, 600/4752 data points at Miami, and 1011/4800 data points at Carberry. The filter contributed between a 4-6 mm increase of cumulative ET over the growing season at all three sites. Most of the data removed were during nights with low wind speeds when ET was close to zero.

Total data gap-filled is outlined in Table 2.10 and shows a greater amount of low-quality data for Glenlea compared to the other 2 sites. Glenlea used a krypton hygrometer for water vapour flux measurements which often yields lower quality data than the infra-red gas analyzers used at Carberry and Miami due to lower sensitivity of the UV detection window when compared to an IRGA (Mauder et al., 2006, Mauder et al., 2007). Therefore, we see more of the data either being removed by thresholds set for water vapour fluxes, flagging of low-quality data using the Mauder and Foken process, or the data not even being collected at Glenlea than the other two sites. Glenlea had a major gap in data due to loss of power at the eddy covariance flux station between June 3, 2018 and June 7, 2018, accounting for 179 consecutively missed half-hour files, which also contributed to the greater amount of missing/low quality data.

Table 2.10 Gap-filled 30-min LE data files for each site over the 2018 growing season.

	Total growing season	**Non-gap-filled**	**Gap-filled**	**Percentage of gap-filled data**
Carberry	4800	3812	988	20.6%
Miami	4752	3913	839	17.7%
Glenlea	4656	2646	2010	43.2%

Uncertainty associated with the IRGAs was minimized with lab and factory calibrations before the growing season and zero checks during the growing season (July 18th for Miami and July 27th for Carberry), as well as close monitoring of signal strength and measured concentrations of water vapour.

Uncertainty with the eddy covariance technique itself was not initially considered as it was assumed to be the actual measurement of ET and all discrepancies between the measured and estimated ET were due to issues with the model. Average random error for LE measured using the eddy covariance method over the growing season calculated by EddyPro v6.2.1 software (LI-COR Inc., 2017) ranged from 6% at Miami to 9% at Carberry. This process is determined by using a cross-correlation function that uses the calculation of "variance of covariance". These percentages do not lead to many differences in ET on a daily basis, but in a multi-year study looking at cumulative ET, it can lead to major differences in measured moisture losses. This error means that adjusting the FAO-56 Penman-Monteith equation to have it more representative of measured ET could be creating more error in the model, especially if there are parts of the growing season where the model represents ET better than the eddy covariance technique.

Even with the corrections to values of LE during the growing season, and the random error assigned to these values, it is still suspected that the eddy covariance method experiences a lack of energy budget closure (Foken, 2008; Leuning et al., 2012). This lack of closure leads to missed measured energy, often more in the form of LE than H.

Energy balance closure was forced for both H and LE with these data by applying a multiplier of 1.39 at Carberry, 1.35 at Miami, and 1.26 at Glenlea to the turbulent fluxes. By forcing energy balance closure, between 20-28% of measured ET was attributed to the forced closure at each site. As this closure method was applied to both H and LE equally and LE is suspected to contribute more to the gap in closure, this method could still be under-representing ET, meaning there is potentially a greater value of ET that is still missed by the current energy balance closure method. This suggests that even though the original FAO-56 Penman-Monteith equation was above the upper 10% error threshold for cumulative measured ET for most of the growing season, the lack of energy balance closure by the eddy covariance technique could be under-representing actual ET, and the original model could produce values of cumulative ET within the 10% error of actual ET. Another assumption that could cause uncertainty in energy balance closure is the assumption that measured available energy is correct. When energy balance closure is forced, the turbulent fluxes are raised so they are equal to available energy. If measured values of available energy are higher than what is actually present in an agroecosystem, turbulent fluxes could be raised too high and represent ET that is larger than what is actually occurring. This would make the gap between measured and estimated ET even greater. Hypothetically, if the energy balance closure issue was fully attributed to over-represented available energy and not missed energy taken by the turbulent fluxes, the unadjusted

FAO-56 Penman-Monteith equation would overestimate ET by as high as 162 mm at Miami, showing that the model cannot represent ET as well as what has been presented in this research.

Mean relative error values outlined in Tables 2.7, 2.8 and 2.9 ranged from 12% to 130% depending on the time period. The largest MRE values are seen in the initial stages of the growing season. As ET at the start of the growing season can be small (less than 0.5 mm day^{-1}) and error at these times in estimation can be 1-3 mm day^{-1}, these differences can yield daily errors far above 100%, which drive up the average MRE for the initial part of the growing season, and subsequently, the whole growing season. Using these values of MRE can be misleading, as errors that are consistently 1 mm day^{-1} yield far greater MRE values at the start of the growing season when ET is naturally lower than during the middle of the growing season. So therefore, root mean square error is a better measure of error that is not based on the size of measured ET.

There is also uncertainty associated with meteorological variables collected, but duplicate measurements of temperature, relative humidity, wind speed, solar radiation and precipitation through different equipment at the same location helped confirm values. Differences between reference ET generated between inputs over the canola and the grassed surface could be associated partly to the difference in equipment used at the eddy covariance flux station and MAWP station.

Leaf area index measurement quality was highly correlated with the environment. Cloudiness, small plants, senesced leaf biomass, and moisture and debris on the equipment lens all decreased accuracy of LAI measurements (LI-COR, 2013). Steps were taken, which are outlined in section 2.3.2.1, to minimize inaccuracies, but the degree measurements of LAI were affected was not analyzed in-depth.

2.7.8 Implications for ET across the Province

Improving estimation techniques of ET by implementing various methods to existing models like the FAO-56 Penman-Monteith equation for Manitoba agroecosystems can improve the understanding of water movement throughout our agricultural fields and the atmosphere. Estimation methods take inputs that are far more readily available in Manitoba to generate ET than measurement methods; as well as, measurement methods like the eddy covariance method might not be able to be done at all geographical locations due to surface roughness, power demands and how remote a location is (Burba & Anderson, 2010). If these improvement methods not only work for canola, but for other prominent crops grown in Manitoba like soybeans (*Glycine max*), spring wheat (*Triticum aestivum*), or maize (*Zea mays*), determination of water losses to the atmosphere can then be more easily determined for more agroecosystems. By measuring the maximum and minimum temperatures, maximum and minimum relative humidity, average wind speed and average incoming solar radiation at a standard weather station, representative ET values for each agroecosystem can be generated with these updates to the model. Producers can then use this information to determine losses of ET from their fields to help make some decisions on whether they should implement water conservation/mitigation strategies for next year. If a producer has irrigation implementation on their farm, they can use this information to determine the most opportune time to irrigate to maximize productivity of their crops. Agronomists can use this information to help diagnose crop productivity problems and suggest management strategies to producers that will help prevent moisture stresses in the future. By improving the FAO-56 Penman-Monteith equation, a readily accessible value of ET can be created and used more broadly.

As varieties of canola that are popularly grown in Manitoba might be different than other provinces, states and countries, being able to characterize popular varieties of crops in Manitoba with the model is really important, as translating a reference ET value to maize grown in only southern states using the FAO-56 crop coefficient would likely not generate ET that represents maize in Manitoba.

2.8 Conclusion

Observing ET over three sites of canola over the 2018 growing season in southern Manitoba helped show the differences between estimated and measured ET for these locations, and where the model falls short in representation of ET. The greatest discrepancies between methods were seen right after seeding, right before harvest, and right before vegetative maturity in fields where plant density was low. Periods right after seeding and right before harvest have the majority of their ET dominated by evaporation (Martel et al., 2018). As evaporation is harder to predict with the model, greater discrepancies occurred when evaporation was the major contributor to ET. Lower plant density of canola only allowed overestimations of actual ET during the period leading up to vegetative maturity as the FAO-56 crop coefficient assumes the canola is at a higher plant density (Gardiol et al., 2003). Canola naturally branches when plant density is low so branching contributes plant biomass that was missing near the start of the growing season, only leaving a lower than typical level of photosynthetically active plant biomass during that period (Angadi et al., 2003), which could be accounted for by LAI and the dynamic crop coefficient.

Adjustments to the model helped minimize these major discrepancies. For the exception of one instance (the water stress coefficient at Glenlea), the R^2 for each individual adjustment improved the representation of estimated actual ET for all 3 sites. The most effective individual method of R^2 improvement for Glenlea and Miami was the dynamic crop coefficient, and the least effective was the water stress coefficient. Carberry had the greatest R^2 improvements with directly measured available energy while the dynamic crop coefficient was the least effective. All three methods combined yielded the greatest improvement to the model for Miami and Carberry (R^2 increased by 0.19 from the unaltered FAO-56 Penman-Monteith model in both instances), while Glenlea had the greatest improvement when all methods were used except the water stress coefficient (R^2 increased by 0.12 from the unaltered FAO-56 Penman-Monteith model). Root mean square error and mean relative error had the greatest improvements when only the measured available energy and dynamic K_c were included at all three sites.

With these improvements to the FAO-56 Penman-Monteith equation for the representation of canola grown in Manitoba, the model can now be used with greater confidence, as the model can more accurately determine actual ET over canola. As cumulative ET from the original FAO-56 Penman-Monteith equation was often outside that upper 10% threshold for measured ET and most of the improvement methods placed the model within the 10% error, there is definite support that the methods improved the model's representation of ET. Along with data produced at many weather stations across the province, the model can help determine the use, consumption and loss to the atmosphere of water in an agroecosystem, which is useful information for producers and people within the agriculture industry who monitor potentials for drought in their fields.

2.9 References

Alberta Agriculture and Forestry. **2013**. Alberta irrigation management model (AIMM). URL https://www1.agric.gov.ab.ca/$department/deptdocs.nsf/all/irr14310.

Allen, R. G., Pereira, L. S., Raes, D., & Smith, M. 1998. Crop evapotranspiration-guidelines for computing crop water requirements. FAO Irrigation and Drainage Paper No. 56, FAO, Rome, Italy.

Angadi, S. V., Cutforth, H. W., McConkey, B. G., & Gan, Y. 2003. Yield adjustment by canola grown at different plant populations under semiarid conditions. *Crop Sci.*, ***43***(4), 1358-1366.

Anthoni, P. M., Freibauer, A., Kolle, O., & Schulze, E. D. 2004. Winter wheat carbon exchange in Thuringia, Germany. *Agric. For. Meteorol.*, ***121***(1-2), 55-67.

Baker, J. M., & Griffis, T. J. 2005. Examining strategies to improve the carbon balance of corn/soybean agriculture using eddy covariance and mass balance techniques. *Agric. For. Meteorol.*, ***128***(3-4), 163-177.

Barr, A. G., Black, T. A., Hogg, E. H., Kljun, N., Morgenstern, K. and Nesic, Z. 2004. Inter-annual variability in the leaf area index of a boreal aspen-hazelnut forest in relation to net ecosystem production. *Agric. For. Meteorol*., **126:** 237-255.

Brutsaert, W. 1982. Evaporation into the atmosphere: Theory. *History, and Applications. D. Reidel*.

Burba, G., & Anderson, D. 2010. A brief practical guide to eddy covariance flux measurements: principles and workflow examples for scientific and industrial applications. Li-Cor Biosciences.

Canola Council of Canada. 2016. Canola grower’s manual. URL https://www.canolacouncil.org/crop-production/canola-grower's-manual-contents/.

Esfahani, M. 2012. Effects of pre-harvest application of paraquat on grain moisture reduction, grain yield and quality of rapeseed (Brassica napus L.) cultivars. *Caspian Journal of Environmental Sciences* ***10***(1), 75.

Fang, X., Minke, A., Pomeroy, J., Brown, T., Westbrook, C., Guo, X., & Guangul, S. 2007. A review of Canadian Prairie hydrology: Principles, modelling and response to land use and drainage change. *Ctr. for Hydro. Rep.*, ***2***. URL https://www.researchgate.net/publication/255632019_A_Review_of_Canadian_Prairie_Hydrology_Principles_Modelling_and_Response_to_Land_Use_and_Drainage_Change.

Finkelstein, P. L., and P. F. Sims. 2001. Sampling error in eddy correlation flux measurements. *Journal of Geophysical Research*, **106**: 3503-3509.

Foken, T. 2008. The energy balance closure problem: an overview. *Ecol. App.*, ***18***(6), 1351-1367.

Gardiol, J. M., Serio, L. A., & Della Maggiora, A. I. 2003. Modelling evapotranspiration of corn (*Zea mays*) under different plant densities. *J. Hydro.*, *271*(1-4), 188-196.

Gervais, M. D. 2009. Assessment of the second generation prairie agrometeorological model's performance for spring wheat on the Canadian Prairies. M.Sc. Thesis. University of Manitoba.

Government of Canada. 2013. Soils of Manitoba. CanSIS report. URL http://sis.agr.gc.ca/cansis/soils/mb/soils.html.

Government of Canada. 2019a. Canadian climate normals. URL http://climate.weather.gc.ca/climate_normals/index_e.html.

Government of Canada. 2019b. Historical data. URL http://climate.weather.gc.ca/historical_data/search_historic_data_e.html.

Knutson, S. 2017. Manitoba soils. Online Interactive Map. GIS 4 Ag Ltd. URL https://mangomap.com/gis4ag/maps/eca07c46-7513-11e4-ad23-22000b2517a0?preview=true#.

Lamb, R.J. 1984. Effects of flea beetles, *Phyllotreta spp.* (Coleoptera: Chrysomelidae), on the survival, growth, seed yield and quality of canola, rape and yellow mustard. *Can. Entomol.* **116**:269-280.

Leuning, R., Van Gorsel, E., Massman, W. J., & Isaac, P. R. 2012. Reflections on the surface energy imbalance problem. *Agric. For. Meteorol.*, ***156***, 65-74.

LI-COR Inc. 2017. EddyPro v6.2.1. Lincoln, Nebraska, USA. URL https://www.licor.com/.

LI-COR. 2013. LAI-2200C plant canopy analyzer instruction manual. LI-COR Inc. Lincoln, Nebraska.

Liu, H. J., & Kang, Y. 2006. Effect of sprinkler irrigation on microclimate in the winter wheat field in the North China Plain. *Agr. Water Manage.*, ***84***(1-2), 3-19.

Martel, M., Glenn, A., Wilson, H., & Kröbel, R. 2018. Simulation of actual evapotranspiration from agricultural landscapes in the Canadian Prairies. *J. Hydro: Regional Studies.*, ***15***, 105-118.

Mathworks. 2013. MATLAB R2013b. Natick, Massachusetts, USA. URL www.mathworks.com/.

Mauder, M., & Foken, T. 2011. Documentation and instruction manual of the eddy-covariance software package TK3.

Mauder, M., Liebethal, C., Göckede, M., Leps, J. P., Beyrich, F., & Foken, T. 2006. Processing and quality control of flux data during LITFASS-2003. *Bound-Lay. Meteorol.*, ***121*****(1)**, 67-88.

Mauder, M., Oncley, S. P., Vogt, R., Weidinger, T., Ribeiro, L., Bernhofer, C., Foken, T., Kohsiek, W., De Bruin, H.A. & Liu, H. 2007. The energy balance experiment EBEX-2000. Part II: Intercomparison of eddy-covariance sensors and post-field data processing methods. *Bound-Lay Meteorol.*, ***123*****(1)**, 29-54.

MAWP. 2018. Manitoba agriculture weather program – Carman. Carman, Manitoba, Canada. URL https://web43.gov.mb.ca/climate/SeasonalReport.aspx.

Microsoft. 2016. Microsoft Excel 2016. Redmond, Washington, USA. URL https://www.microsoft.com/en-ca.

Moncrieff, J. B., J. M. Massheder, H. de Bruin, J. Ebers, T. Friborg, B. Heusinkveld, P. Kabat, S. Scott, H. Soegaard, & A. Verhoef. 1997. A system to measure surface fluxes of momentum, sensible heat, water vapor and carbon dioxide. *J. Hydro.*, **188-189**: 589-611.

Moncrieff, J., Clement, R., Finnigan, J., & Meyers, T. 2004. Averaging, detrending, and filtering of eddy covariance time series. In *Handbook of Micrometeorology*. (pp. 7-31). Springer, Dordrecht.

North Dakota Agricultural Weather Network (NDAWN). 2018. Canola development and growing degree days (GDD). URL https://ndawn.ndsu.nodak.edu/help-canola-growing-degree-days.html.

Papale, D., Reichstein, M., Aubinet, M., Canfora, E., Bernhofer, C., Kutsch, W., Longdoz, B., Rambal, S., Valentini, R., Vesala, T. & Yakir, D. 2006. Towards a standardized processing of net ecosystem exchange measured with eddy covariance technique: algorithms and uncertainty estimation. *Biogeosciences*, ***3*****(4)**: 571-583.

Penman, H. L. 1948. Natural evaporation from open water, bare soil and grass. *Proc. R. Soc. A. Math. Phys. Sci.*, ***193***(1032), 120-145.

R Core Team. 2018. R: A language and environment for statistical computing. R Foundation for Statistical Computing, Vienna, Austria. URL https://www.R-project.org/.

Santanello Jr, J. A., & Friedl, M. A. 2003. Diurnal covariation in soil heat flux and net radiation. *J. of Appl. Meteorol.*, ***42***(6), 851-862.

Verstraeten, W., Veroustraete, F., & Feyen, J. 2008. Assessment of evapotranspiration and soil moisture content across different scales of observation. *Sensors*, ***8***(1), 70-117.

Vickers, D., & Mahrt, L. 1997. Quality control and flux sampling problems for tower and aircraft data. *J. of Atmos. Ocean. Tech.*, ***14***(3), 512-526.

Wilson, K., Goldstein, A., Falge, E., Aubinet, M., Baldocchi, D., Berbigier, P., Bernhofer, C., Ceulemans, R., Dolman, H., Field, C. & Grelle, A. 2002. Energy balance closure at FLUXNET sites. *Agric. For. Meteorol.*, ***113***(1-4), 223-243.

3 OVERALL SYNTHESIS

Estimation of ET can be done using the FAO-56 Penman-Monteith equation and can be used as a key component of determining the rate of water vapour leaving a soil/plant system to the atmosphere (Allen et al., 1998). Discrepancies between model-generated ET and measured actual ET over the same agroecosystem suggest issues with how canola grown in Manitoba currently is represented by the model. This research project attempts to minimize these discrepancies with different model adjustments to improve the reliability of this model for ET in canola-based agroecosystems across the province. This synthesis will summarize the thesis and provide reflection and insight into the results, as well as the potential impact this research has for future studies, and ET determination across the province.

3.1 Summary

The eddy covariance technique was used to determine water vapour fluxes at three sites across Manitoba, one site 2 km north of Carberry at the Canada Manitoba Crop Diversification Centre, one site west of Miami along the South Tobacco Creek, and one location on the University of Manitoba's Trace Gas Manitoba Greenhouse Gas Field Emission Site close to Glenlea. Additionally, temperature, relative humidity, wind speed and incoming solar radiation were measured at these sites to also estimate ET through the FAO-56 Penman-Monteith equation. A comparison between the measured and estimated ET was done over the 2018 growing season, with each field season lasting 97-100 days over the span of May 10th to August 22nd. Management strategies differed for each field system and were controlled by the producer.

The objectives of the study were to compare estimated and measured ET over the growing season and determine where major discrepancies lied in their comparison. It was also an objective to determine if incorporating 3 different adjustments to the model would minimize differences between estimated and measured ET. The final objective was to see if the estimation technique differed largely when meteorological data were taken in-crop or over a nearby meteorological station with a grass surface.

The largest discrepancies between the estimated and measured ET were during the periods right after seeding, right before harvest and right before vegetative maturity in fields with lower plant densities. As periods right after seeding and right before harvest have minimal photosynthetically active plant biomass present, the majority of ET is in the form of evaporation (Martel et al., 2018). As evaporation is largely impacted by environmental factors, and Penman's evaporation component of the equation was determined for an open-water body with a surface resistance different from an agricultural field, evaporation is harder to model using the Penman-Monteith equation than transpiration for an agroecosystem. When ET was mostly dominated by transpiration during the middle of the growing season, agreement between measured and estimated ET was better than during the beginning and end of the growing season (Martel et al., 2018). At any point in the growing season where biomass development is not as expected for a growth stage, the model will have problems representing ET because the equation uses a constant canopy conductance (Allen et al., 1998; Gardiol et al., 2003). During these points in the growing season where the canopy was not properly represented by the unadjusted equation, using a dynamic crop coefficient generated by leaf area index measurements improved agreement to a high degree.

The improvement methods to the model included incorporating directly measured available energy (net radiation – ground heat flux), using a dynamic crop coefficient generated from leaf area index values and a water stress coefficient. Changes in R^2, RMSE and MRE showed that measured available energy and the dynamic crop coefficient improved the modelled ET at every site. The water stress coefficient only improved the model's R^2 at Miami and Carberry, every other statistic was worsened with the incorporation of the model improvement. Combinations of improvement methods showed that the best combination of model improvements was using the measured available energy and dynamic crop coefficient only.

Minimal differences were seen between ET estimated using meteorological values generated over the crop compared to over the intended grass surface at the Carberry site. Any differences in results were attributed to irrigation events in the field that did not occur over the grass surface and their effect on temperature and relative humidity (Liu & Kang, 2006).

3.2 Significance

This project helped analyze the existing FAO-56 Penman-Monteith equation and validate it over Southern Manitoba's canola-based agroecosystems. This showed how canola was represented by the model and its short-comings when using the model to represent canola grown currently in Manitoba. As canola is a major crop grown in Manitoba, and the varieties grown currently in Manitoba are different than varieties grown in the Central United States in the 1990's where/when the model was validated (Allen et al., 1998), ensuring that the model can represent ET in these systems means it can be used with greater confidence in the future. This project also brings to attention areas where the model represents canola to a lesser extent, which leads researchers or producers who use this model to represent ET in their fields to understand how accurate their estimations of ET are depending on the point in the growing season. The project also outlined an issue with the FAO-56 Penman-Monteith model representing actual ET when evaporation was the prominent contributor to total ET (right after seeding and right before harvest) that could be considered as a potential point of improvement for the future.

This project showed that the incorporation of three different methods for the most part improved the model's ability to represent actual ET. With this information and the investments of additional equipment, information gathered at weather stations across the province can be used with greater confidence that they are estimating actual ET as accurately as possible.

The project also showed that inputs for the FAO-56 Penman-Monteith equation were not largely affected by being measured within the field system or over a nearby grass surface when generating values of reference ET. The proper grass surface of 0.12 cm, 70 s m^{-1} surface resistance and a 0.23 albedo is not too important when determining these values to generate reference ET, and using meteorological values generated in a canola field in the model could be done if the proper grass surface cannot be measured.

Overall, this research is a step forward in understanding ET dynamics in different agroecosystems, and helps give the ability to determine ET correctly to a greater audience. This makes mapping water movement easier for canola producers on the prairies, and can starting point for improving estimations for other major crops grown on the prairies.

3.3 Improvements

The major improvement to the project would be to increase consistency between sites. Consistency in equipment, mainly the gas analyzer, would help minimize uncertainty between sites for water vapour fluxes. The use of a krypton hygrometer at one site that uses ultraviolet light to analyze water vapour concentrations and the use of infra-red gas analyzers at the other two sites leads to possible differences in abilities to measure ET. Potential differences in measured ET results could have arose from using an open-path gas analyzer at Glenlea and Miami, but an enclosed-path gas analyzer at Carberry (Halswanter et al., 2009). Differences between open-path and enclosed-path gas analyzers determination of ET have been explored at the Carberry location (APPENDIX I). Linear regressions between open-path (y-axis) and enclosed-path (x-axis) gas analyzers in this study showed R^2 values for LE of 0.91 and a slope of 0.93, which shows the LE values from the two analyzers were similar, but some error could be attributed to differences in gas analyzers. There was also inconsistency in agronomic practices and harvest methods. It was not suspected that these factors could have greatly contributed to the difference in ET between the 3 sites, but eliminating these factors as variables could have ensured that they would not play a role in site differences. Although confidence in ET measurements taken at the sites throughout the 2018 growing season was adequate as random error associated with latent heat flux measurements ranged between 6-9%, general patterns in daily ET between the three sites were similar (Figure 2.1) and average daily ET between the three sites ranged from 3.35 and 3.38 mm day^{-1}.

Even though each site was visited once a week, more frequent visits would have benefitted the mapping of leaf area index and crop staging to be used for the dynamic crop coefficient. As some days were not ideal to measure LAI because of the weather, there were limited days where LAI could be used. This left only 5 days of measurements to derive curves to represent LAI for the whole growing season to be in the case of Glenlea. Key crop stages were missed as the changes could not be picked up clearly by trail cam pictures taken 4 times a day, and only weekly site visits were done.

More supplementary information should have been taken at site visits in addition to leaf area index, crop height and crop staging. Information about plant density, crop surface coverage and biomass samples should have been taken on a weekly or biweekly basis to help characterize the development of canola before LAI values could be accurately depicted using the LAI-2200.

LAI could not be recorded until a certain height of the canopy was reached (4x the leaf width), so prior to that, no LAI values were taken. Even though ET at these stages of development were minimal, these missing values could have made the curve fit even better and improved the model's estimation of ET to a greater extent. Additionally, stomatal conductance could have been measured on photosynthetically active plant biomass or could have been back-calculated using information collected from the flux towers to generate a canopy conductance that was more representative of the plant biomass in the field to help characterize plant density in addition to LAI measurements.

Another potential area of improvement would be with the analysis of data and what information was used to determine if the model was improved by incorporating adjustments. Linear regressions were used mainly to determine the success of the improvement method, with the addition of cumulative ET values throughout the growing season as a smoothed depiction of improvements. As linear regressions were based on a comparison of measured and estimated ET on a daily basis, and statistics like R^2 and MRE based on linear regressions show values of dispersion, it is harder to conclude that agreement between measured and estimated ET improved as much as dispersion between measured and estimated ET improved. Cumulative ET totals for each improvement method in Figures 2.8, 2.9 and 2.10 show how the improvement method changed ET throughout the growing season. If this was relied on as the primary source of information to determine the most improved model, the conclusions would be different as the improvement method resulting in the closest value of cumulative growing season ET to measured ET was not the model with the greatest improvements in R^2, RMSE and MRE for every site.

A better analysis of rooting depth would have been beneficial for the development of an accurate water stress coefficient. The presence of water stress was predicted to cause a lack of ET during the end of the growing season at Miami, but the water stress coefficient did not express this. As canola's maximum assumed rooting depth by the Canola Council of Canada to be 1.4 m, the generation of the water stress coefficient was based on this assumption (Canola Council of Canada, 2016). The water stress coefficient uses rooting depth to show the amount of accessible water in the soil, so when the maximum rooting depth was assumed to be 1.0 m, far less soil moisture was accessible and severe water stress was apparent (APPENDIX II). Based on this information, it is likely that the actual maximum rooting depth was between 1.0 m and 1.4 m. The degree the canola was stressed based on ET values showed that measured ET at the end of the growing season was between estimated ET values with the applied water stress coefficients at both maximum rooting depths. If actual measurements of rooting depth were done, there would be a greater confidence with the true maximum rooting depth to apply to the water stress coefficient, yielding greater confidence for the coefficient's representation of water stress.

A large area of uncertainty when dealing with eddy covariance data is the lack of energy balance closure. It is stated that energy-closure adjustments are necessary for eddy covariance measurements of ET, but how adjustments should be applied is unknown (Barr et al., 2012). Multiple studies have found ways to limit the problem of energy balance closure. There is attenuation of water vapour in sampling lines of closed-path IRGAs that contribute to large latent heat flux losses which was avoided by these eddy covariance systems by using open-path and enclosed-path gas analyzers (Fratini et al., 2012). Incorporating heat storage terms, especially during daytime periods is vital for improving energy balance closure, which was done with data collected at the eddy covariance systems with this project (Kutikoff et al., 2019). But issues still persist as measured ET at the three sites studied in this research had 20-28% of the ET attributed to forced energy balance closure. This adjustment to measured ET is quite large and makes the reliability of the measurements questionable. As current energy balance closure procedures require assumptions such as assuming measured available energy is representative of actual available energy, and that latent and sensible heat fluxes contribute equally to the gap in turbulent fluxes and available energy, there is even greater uncertainty brought into energy balance closure. The largest contributor to the energy balance closure problem is the fact that large amounts of energy transport in large eddies is missed by the eddy covariance system because the towers are too short, as these larger eddies exist above the towers in the atmosphere (Foken, 2008). Being able to account for these larger eddies through direct measurements instead of using assumptions would be an improvement to the representation of turbulent fluxes and ET. Even though there has been work done to minimize the energy balance closure problem, there is still work needed to be done to fully understand and eliminate the gap between turbulent fluxes and available energy. The energy balance closure problem needs to be improved to increase the reliability of both eddy covariance ET and the models that use eddy covariance to be validated.

3.4 Future Studies

As this study was the first study to validate and make improvements to the FAO-56 Penman-Monteith equation for a specific crop of canola in Southern Manitoba, this study could be done to validate the model in other cropping systems. Major crops grown in Manitoba like spring wheat (*Triticum aestivum*), soybeans (*Glycine max*) and maize (*Zea mays*) could be looked at, as specifically soybeans and maize grown in Manitoba differ largely from soybeans and maize grown in central United States where the model was initially created to represent.

Manitoba soybeans and maize complete their life cycle in a much shorter time period (Cloutier, 2017; Hamel & Dorff, 2015), so this would affect the patterns of ET emitted by a field of soybeans in Manitoba compared to the central United States. To ensure the FAO-56 Penman-Monteith equation could represent ET in commonly grown crops in Manitoba, the model should be tested such as in Martel et al., (2018).

As this project only looked at canola grown at 3 sites across Manitoba during one growing season, further projects could look at canola grown at different sites over multiple growing seasons. One year's data is good to help validate the FAO-56 Penman-Monteith equation, but additional years can help distinguish if the model truly represents ET from canola, especially if the growing seasons are different (cool and wet versus hot and dry).

Using leaf area index to characterize the development of the crop in place of a crop coefficient could be a method of determining ET in polycultural systems, unique crops or fields of pasture with inconsistent patterns of plant density. As this method characterizes the total photosynthetically active biomass, it can be used to determine patterns of ET for systems that do not have a crop coefficient already for the FAO-56 Penman-Monteith equation.

3.5 References

Allen, R. G., Pereira, L. S., Raes, D., & Smith, M. 1998. Crop evapotranspiration-guidelines for computing crop water requirements. FAO Irrigation and Drainage Paper No. 56, FAO, Rome, Italy.

Barr, A. G., Van der Kamp, G., Black, T. A., McCaughey, J. H., & Nesic, Z. 2012. Energy balance closure at the BERMS flux towers in relation to the water balance of the White Gull Creek watershed 1999–2009. *Agric. For. Meteorol.*, ***153***, 3-13.

Canola Council of Canada. 2016. Canola grower's manual. URL https://www.canolacouncil.org/crop-production/canola-grower's-manual-contents/.

Cloutier, J., 2017. Soy story: a short history of *Glycine max* in Canada. Statistics Canada.

Foken, T. 2008. The energy balance closure problem: an overview. *Ecol. App.*, ***18***(6), 1351-1367.

Fratini, G., Ibrom, A., Arriga, N., Burba, G., & Papale, D. 2012. Relative humidity effects on water vapour fluxes measured with closed-path eddy-covariance systems with short sampling lines. *Agric. For. Meteorol.*, ***165***, 53-63.

Gardiol, J. M., Serio, L. A., & Della Maggiora, A. I. 2003. Modelling evapotranspiration of corn (*Zea mays*) under different plant densities. *J. Hydro.*, ***271***(1-4), 188-196.

Hamel, M., Dorff, E. 2015. Corn: Canada's third most valuable crop. Statistics Canada.

Kutikoff, S., Lin, X., Evett, S., Gowda, P., Moorhead, J., Marek, G., Colaizzi, P., Aiken, R., & Brauer, D. 2019. Heat storage and its effect on the surface energy balance closure under advective conditions. *Agric. For. Meteorol.*, ***265***, 56-69.

Liu, H. J., & Kang, Y. 2006. Effect of sprinkler irrigation on microclimate in the winter wheat field in the North China Plain. *Agr. Water Manage.*, ***84***(1-2), 3-19.

Martel, M., Glenn, A., Wilson, H., & Kröbel, R. 2018. Simulation of actual evapotranspiration from agricultural landscapes in the Canadian Prairies. *J. Hydro: Regional Studies.*, ***15***, 105-118.

APPENDICIES

I. Comparing Open-Path and Enclosed-Path Eddy Covariance Systems

Introduction

Infra-red gas analyzers (IRGAs) and krypton hygrometers are used in eddy covariance systems to determine water vapour concentrations. The most common varieties of IRGAs can be considered either open-path or closed-path. The main difference between the two methods is the location of the optical analysis of these gas concentrations (Halswanter et al., 2009). Open-path IRGAs measure concentrations of gases within eddies along an optical path exposed to the elements. Closed-path IRGAs draw air along a sampling tube, where concentrations of gases are measured along an optical cell within the IRGA itself. In order to draw air along a sampling tube, a closed-path IRGA requires a pump, resulting in greater power consumption. Greater power demands are not ideal for most studies in remote locations with limited power. Open-path systems although are more impacted by condensation, rain, dew, frost, snow, dust and other debris as their optical lenses are exposed to the environment. An enclosed-path IRGA minimizes the negative effects of both methods mentioned as it has a closed-path optical cell that can be mounted at the same level as its intake tube. This limits the distance of the sampling tube, minimizing power demands for a pump and decreases the sensitivity of the system to environmental conditions.

The purpose of this exercise was to compare data collected by different EC systems to observe how differences in equipment and processing techniques effect the outcome of flux calculations for latent heat (LE) and sensible heat (H).

Materials and Methods

The comparison took place at the Canada-Manitoba Crop Diversification Centre (49.91^{o}N, 99.35^{o}W; 409 m a.s.l) approximately 4 km north of the town of Carberry, MB from July 25, 2018 to August 2, 2018. Carberry can be described as having a humid, cool continental climate, with it being given the Köppen climate classification of Dfb. This suggests that Carberry does not necessarily have a dry winter or summer, and that the average temperature of the warmest month is less than 22°C. The average last spring frost is May 16-19 and the average first fall frost is September 11-16. Precipitation is greatest from May to August and there is around 455 mm of precipitation year-round. The 2018 growing season had canola (*Brassica napus*) and during the time of this comparison, the canola was in the seed development stage.

An additional comparison between the same open-path system used in Carberry and an open-path system approximately 9.5 km southwest of Miami, MB from August 2, 2018 to August 17, 2018 was conducted. Like Carberry, Miami is given a Köppen climate classification of Dfb. The average last spring frost is May 16-19 and the average first fall frost is September 16-21. Precipitation is greatest from May to August and there is around 484 mm of precipitation year-round. The canola at this point was in the senescence stage.

The same permanent enclosed-path eddy covariance system at Carberry and permanent open-path eddy covariance system at Miami that were outlined in section 2.5.2.1 were used in this experiment. The semi-permanent open-path eddy covariance system was set-up and recorded good quality data at the Carberry site over the span of July 24, 2018 – August 2, 2018 and at the Miami site over the span of August 2, 2018 – August 17, 2018. This system consisted of an ultrasonic anemometer (model 81000, R. M. Young Company, Traverse City, MI) and an open-path krypton hygrometer (model KH20, Campbell Sci., Logan, UT). Both the permanent and semi-permanent eddy covariance systems were mounted at 2.25 m, which was over a meter higher than the canola's average height. The instrumentation was oriented directly west to capture the prevailing winds. Raw data for both systems were processed using the same process done in Chapter 2 (refer to section 2.5.3 for greater details in data processing). The only major difference in processing was that there was no gap-filling or forced energy balance closure completed. Data for H and LE that was both corrected and uncorrected with a low and high frequency spectral correction factor were analyzed. Fluxes were compared with MATLAB R2013b software (Mathworks, 2013) for H and LE using a linear regression.

Results and Discussion

There was close agreement between semi-permanent open-path and permanent enclosed-path systems when looking at both H and LE at Carberry. Figure I.1 shows the R^2 between the permanent enclosed-path system and the semi-permanent open-path system for LE is 0.92, which is less than the R^2 at the same site for H which was 0.98 (Figure I.3). Exact reasons for differences are unclear. It is thought that closed-path methods yield greater values of LE compared to open-path during periods of high temperatures and low relative humidity (Halswanter et al., 2009). A consistent pattern of higher closed-path measurements of LE was not seen in comparison to the semi-permanent open-path system during periods of higher temperature and lower relative humidity though. The slope of the regression equation for both H and LE at Carberry was close to 1, suggesting that values generated by the permanent enclosed-path system and the semi-permanent open-path system were equal to each other.

Figures I.5 and I.7 show there were similar results seen between the permanent open-path gas analyzer and the semi-permanent open-path gas analyzer for LE and H at Miami. The dispersion between the two systems was an R^2 value between 0.97 and 0.99. The slopes of the regression were close to 1 again, although the slope for LE was slightly greater at 1.12, which suggests slightly higher values generated by the semi-permanent open-path system.

Uncorrected H and LE at both sites didn't result in large differences in R^2 between the permanent and semi-permanent systems, with the largest difference in R^2 between the corrected and uncorrected data being 0.01 (Figure I.2, I.4, I.6, and I.8). Slopes did change to a greater extent for LE as without the correction they decreased from 1.00 to 0.93 at Carberry and from 1.12 to 0.99 at Miami (Figure I.2 and I.6).

Overall there was close correspondence between open and enclosed-path eddy covariance systems over the span of July 24 to August 2, 2018 for H and LE at Carberry. There was also close correspondence between the permanent and semi-permanent open-path gas analyzers over the span of August 2 to August 17, 2018 for H and LE at Miami. These comparisons helped confirm the reliability of all equipment set-ups tested in measuring components of the eddy covariance method at Carberry and Miami.

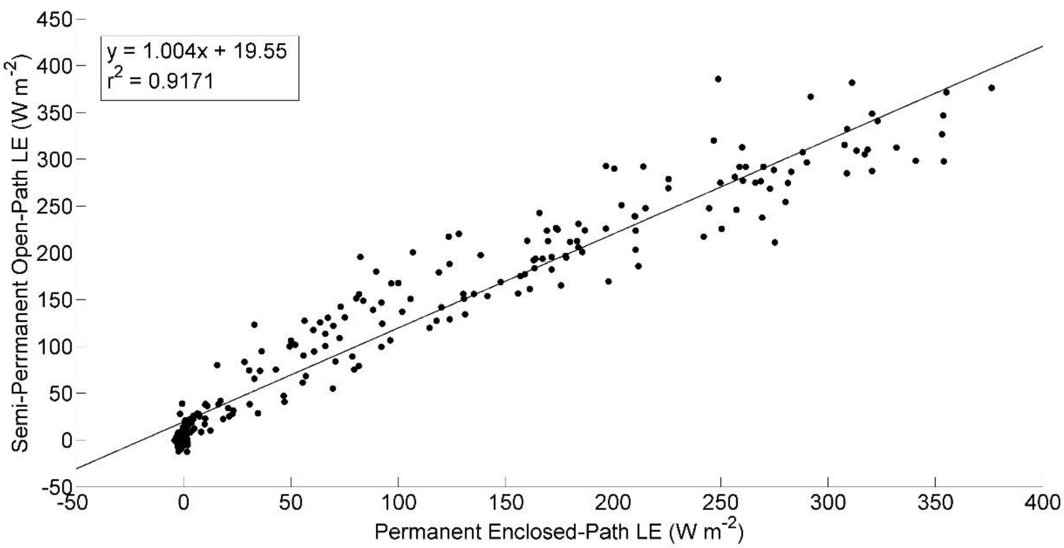

Figure I.1 Comparison of measured corrected latent heat (LE) fluxes between an enclosed path and open-path eddy covariance system over canola at the Carberry site from July 24, 2018 to August 2, 2018.

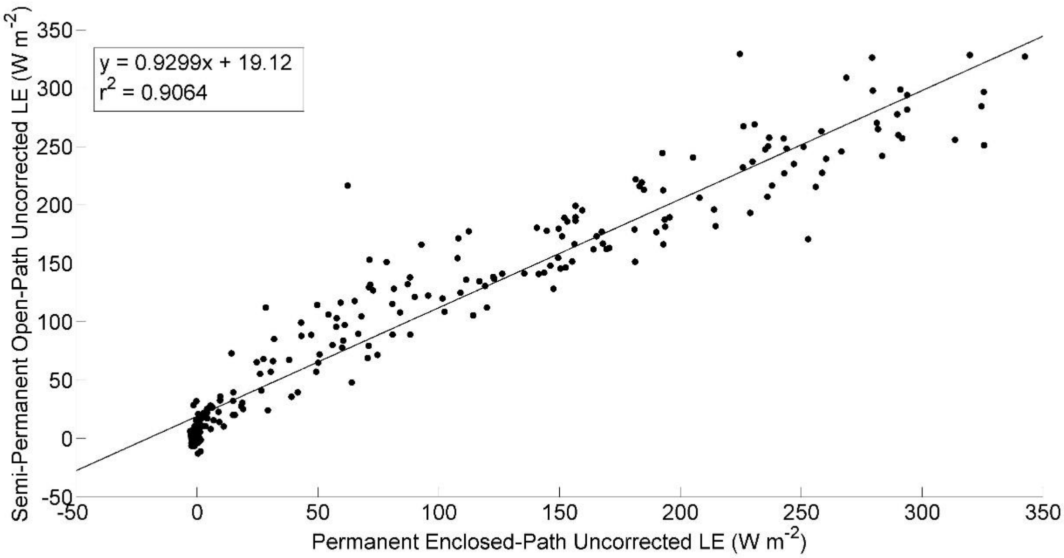

Figure I.2 Comparison of measured uncorrected latent heat (LE) fluxes between an enclosed path and an open-path eddy covariance system over canola at the Carberry site from July 24, 2018 to August 2, 2018.

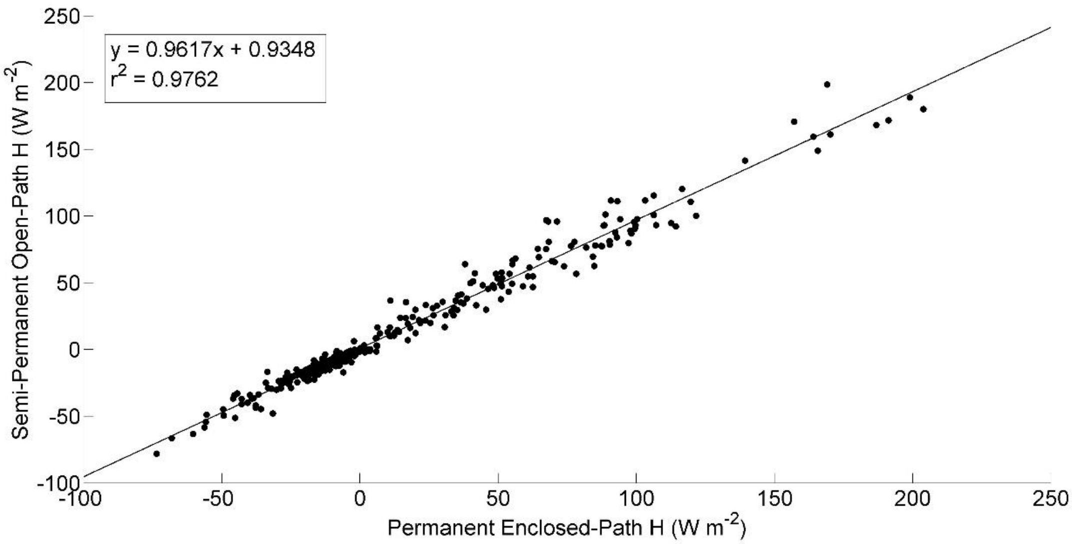

Figure I.3 Comparison of measured corrected sensible heat (H) fluxes between an enclosed-path and open-path eddy covariance system over canola at the Carberry site from July 24, 2018 to August 2, 2018.

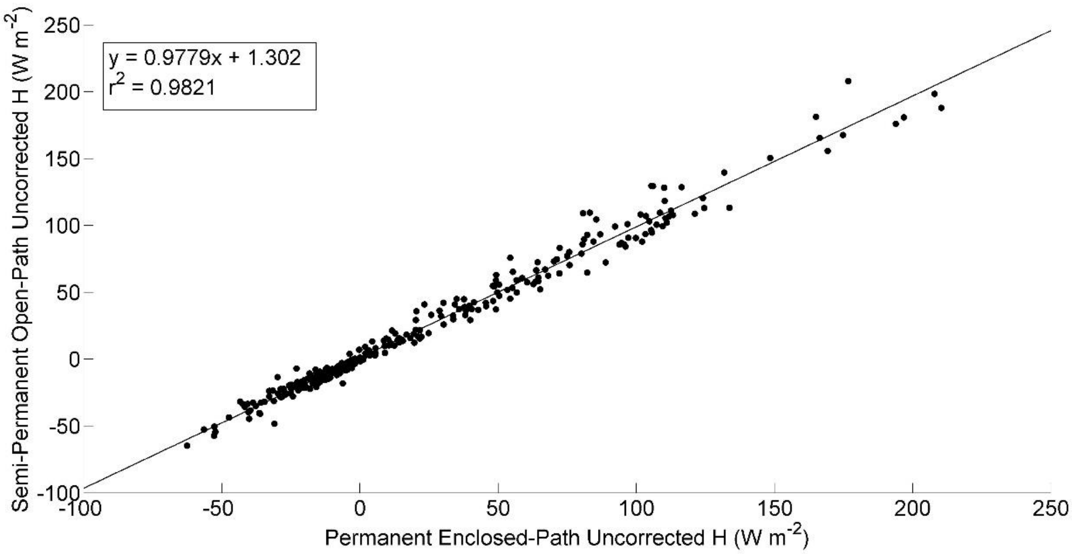

Figure I.4 Comparison of measured uncorrected sensible heat (H) fluxes between an enclosed-path and open-path eddy covariance system over canola at the Carberry site from July 24, 2018 to August 2, 2018.

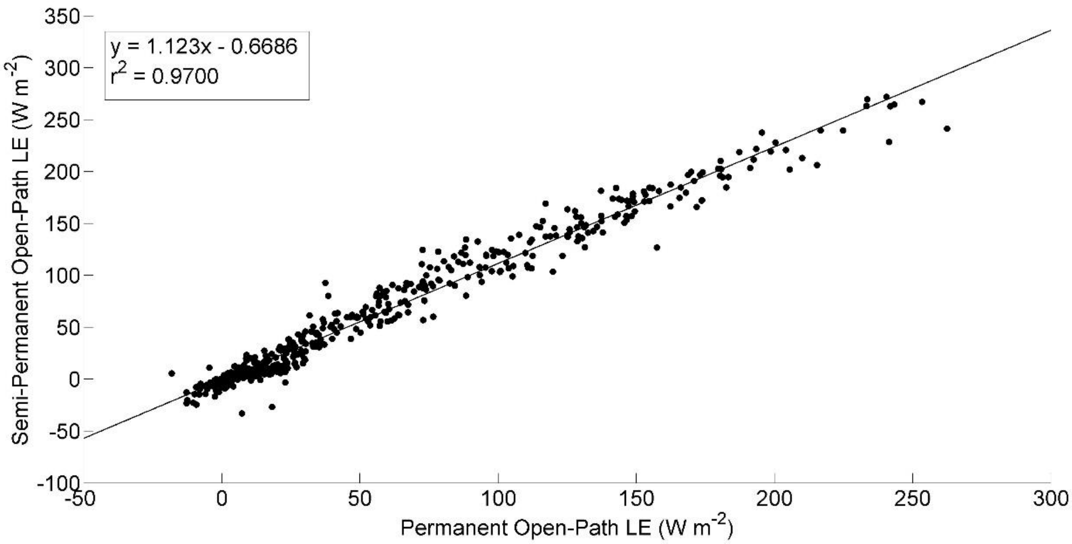

Figure I.5 Comparison of measured corrected latent heat (LE) fluxes between a permanent and semi-permanent open-path eddy covariance system over canola at the Miami site from August 2, 2018 to August 17, 2018.

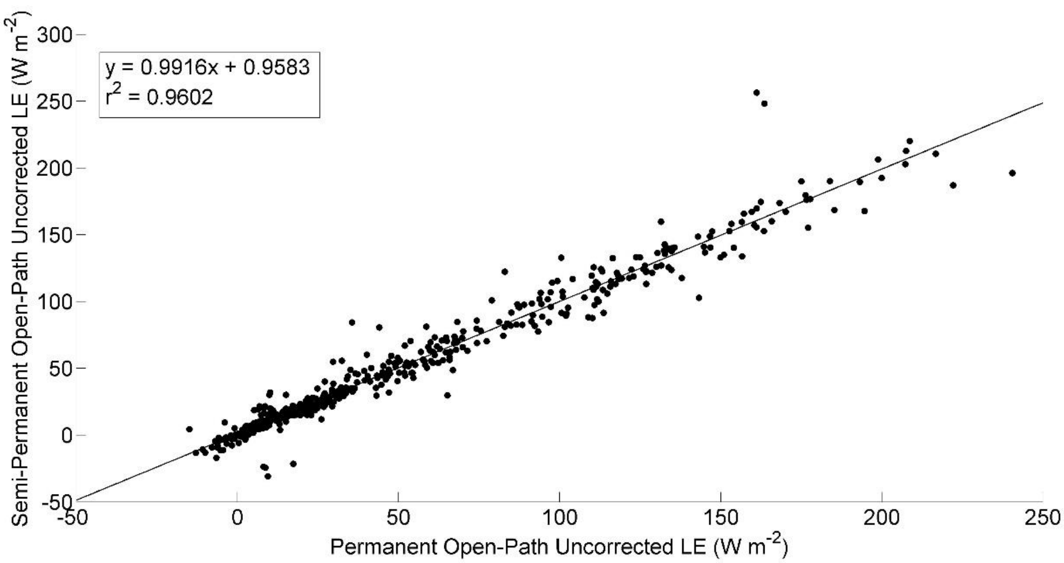

Figure I.6 Comparison of measured uncorrected latent heat (LE) fluxes between a permanent and semi-permanent open-path eddy covariance system over canola at the Miami site from August 2, 2018 to August 17, 2018.

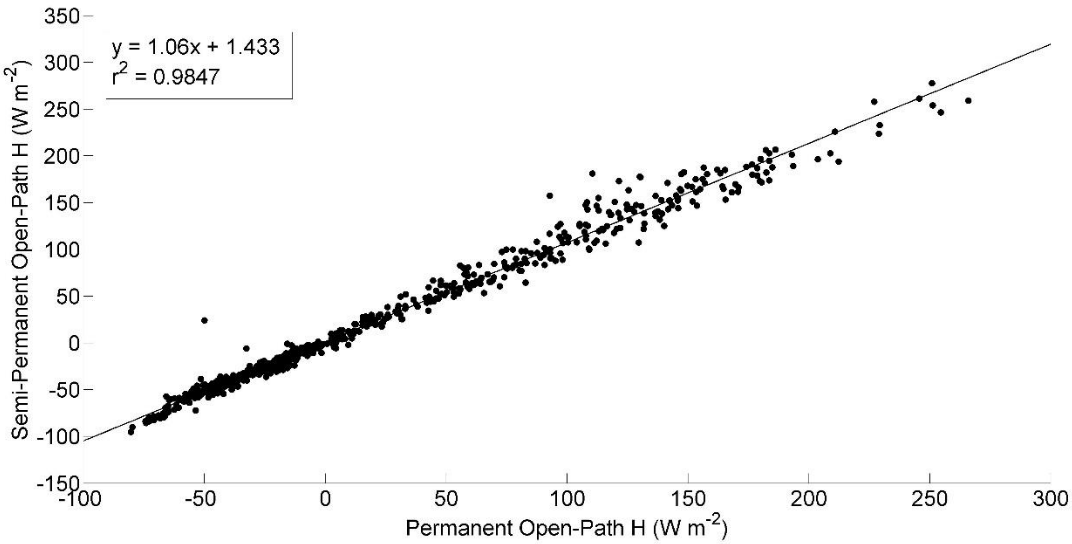

Figure I.7 Comparison of measured corrected sensible heat (H) fluxes between a permanent and semi-permanent open-path eddy covariance system over canola at the Miami site from August 2, 2018 to August 17, 2018.

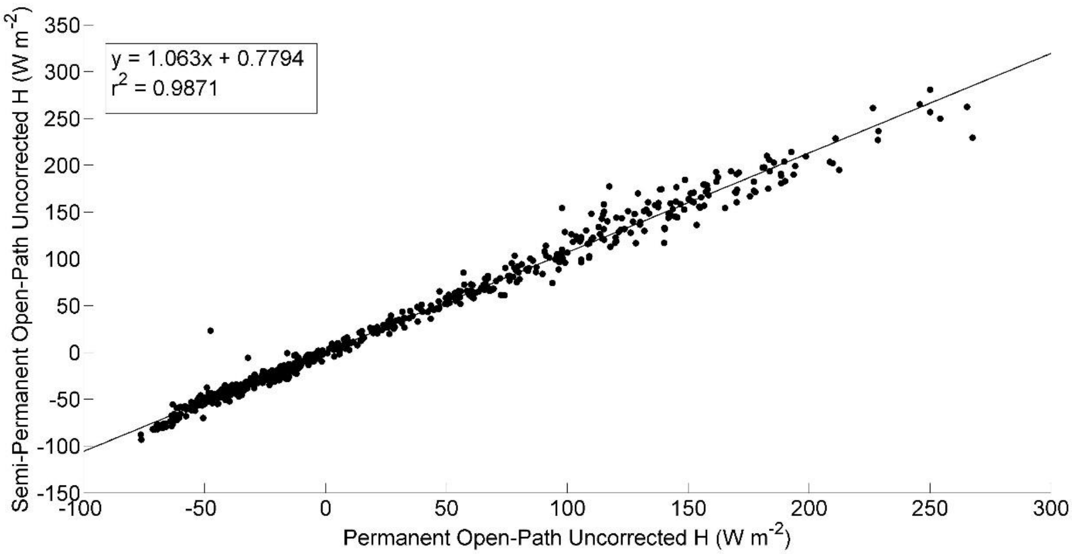

Figure I.8 Comparison of measured uncorrected sensible heat (H) fluxes between a permanent and semi-permanent open-path eddy covariance system over canola at the Miami site from August 2, 2018 to August 17, 2018.

References

Haslwanter, A., Hammerle, A., & Wohlfahrt, G. 2009. Open-path vs. closed-path eddy covariance measurements of the net ecosystem carbon dioxide and water vapour exchange: A long-term perspective. *Agric. For. Meteorol.*, ***149***(2), 291-302.

Mathworks. 2013. MATLAB R2013b. Natick, Massachusetts, USA. URL www.mathworks.com/.

II. Estimating Canola (*Brassica napus*) Rooting Depth using the Water Stress Coefficient

Measuring maximum rooting depth is difficult in most rooting systems, especially in clay soils. Collecting root biomass samples is challenging as roots can be damaged or lost during sample collection and cleaning. Being able to estimate rooting depths of canola using soil moisture data can be done if sensors are present in the field at multiple depths. Observing the volumetric water content at different depths can give insight as to the rooting depth. For example, if there is a noticeable discharge of moisture at the 50 cm depth but no similar pattern of decreased moisture at the 100 cm depth, the root system has likely approached or is approaching the 50 cm depth, but has not reached the 100 cm depth. But in fields without the ability to measure volumetric moisture content at various depths on an hourly basis, there is not much information that can be used to determine rooting depth.

The Canola Council of Canada suggests the average maximum rooting depth for canola is 1.4 m (Canola Council of Canada, 2016), but rooting depth is often influenced by factors including available moisture and soil type. By generating a water stress coefficient to improve estimates of ET in Chapter 2, a potential method of analyzing rooting depth based on the water balance of an agroecosystem was observed.

To generate a water stress coefficient, a rooting depth must be assumed for canola. For the purposes of Chapter 2, the maximum rooting depth was assumed to be 1.4 m (Canola Council of Canada, 2016). No water stress was seen during the growing season for the exception of the first 3 days after emergence. It was suspected that the canola at Miami was under stress induced by flea beetles (*Phyllotreta cruciferae*) present at the start of the growing season or the lack of available moisture, so not finding any stress from the water stress coefficient led to further analysis of the coefficient. Water stress coefficients were then generated for a canola crop that only reached 1.0 m rooting depth. With this change, the water stress coefficient showed that there was stress caused by a lack of available water starting on July 17, 2018 and went to the end of the growing season (Figure II.1). The stress outlined by a water stress coefficient tied to a maximum rooting depth of 1.0 m was far greater than what was experienced in the field. During the last third of the growing season, it was apparent that the water stress coefficient generated from a maximum rooting depth of 1.4 m overestimated ET and the water stress coefficient generated from a maximum rooting depth of 1.0 m underestimated ET. This would suggest that a maximum rooting depth between 1.0 and 1.4 m would make using the water stress coefficient provide the best agreement between actual ET, suggesting that the maximum rooting depth of the canola at the site was between 1.0 and 1.4 m.

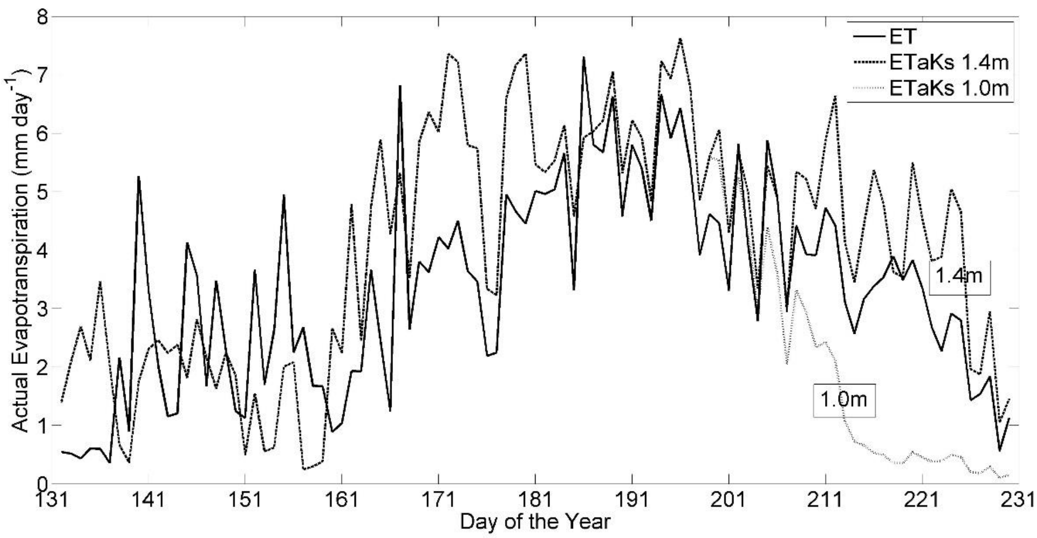

Figure II.1 Differences in predicted maximum rooting depth for water stress coefficients and how they compare to actual measured ET (ET) when applied to estimated ET at 1.4 m rooting depth (ETa K_s 1.4m) and 1.0 m rooting depth (ETa K_s 1.0m) at the Miami location.

References

Canola Council of Canada. 2016. Canola grower’s manual. URL https://www.canolacouncil.org/crop-production/canola-grower's-manual-contents/.